

TOSHIBA CORPORATION

1-1, SHIBAURA 1-CHOME, MINATO-KU TOKYO 105-8001, JAPAN

TOS-CR-4S-2012-0006

Project Number 0760

September 26, 2012

U.S. Nuclear Regulatory Commission
Document Control Desk
Washington, DC 20555-0001

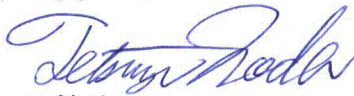
Subject: Submittal of Technical Report "Validation of 4S Safety Analysis Code SAEMKON for Loss of Offsite Power Event"

Enclosed is a copy of the non-proprietary technical report "Validation of 4S Safety Analysis Code SAEMKON for Loss of Offsite Power Event" for the 4S (Super-Safe, Small and Simple) reactor plant that is currently the subject of a pre-application review among NRC, Toshiba and its 4S affiliates including Japan's Central research Institute for Electric Power Industry (CRIEPI).

The pre-application review for the 4S reactor commenced in the fourth quarter of 2007. Pre-application review meetings were held among NRC, Toshiba and the 4S affiliates in October 2007, and February, May and August 2008.

If you have any questions regarding this document, please contact Mr. Tony Greci of Westinghouse at (623) 271-9992, or grecit@westinghouse.com.

Very truly yours,



Tetsuya Noda
Senior Manager, Plant Project Engineering Department
Nuclear Energy Systems & Services Division, Power Systems Company
Toshiba Corporation

Enclosures: Technical Report "Validation of 4S Safety Analysis Code SAEMKON for Loss of Offsite Power Event"

cc: Michael Mayfield (NRO/DNRL)
Tom Kevern (NRO/DNRL)
Bill Reckley (NRO/DNRL)
Don Carlson (NRO/DNRL)
Nobuyuki Ueda (CRIEPI)
Tony Greci (Westinghouse)
Dewey Olinski (Westinghouse)
Abdellatif M. Yacout (Argonne National Laboratory)

D104
NRD

Document Number: AFT-2012-000063rev003(0)

PSN Control Number: PSN-2012-1227

**Validation of 4S Safety Analysis Code
SAEMKON
for Loss of Offsite Power Event**

September 2012

TOSHIBA CORPORATION

TABLE OF CONTENTS

Section	Title	Page No.
	LIST OF TABLES	ii
	LIST OF FIGURES	iii
	LIST OF FIGURES	iii
	LIST OF ACRONYMS AND ABBREVIATIONS	v
1.	INTRODUCTION	1-1
1.1.	4S Plant Design	1-1
1.2.	Safety Analysis Code SAEMKON	1-3
2.	VALIDATION STRATEGY	2-1
2.1.	Events Selection	2-1
2.2.	Target Phenomena	2-2
2.3.	Test Type	2-5
2.4.	Acceptance Criteria	2-7
3.	VALIDATION RESULTS	3-1
3.1.	Separate Effects Tests	3-1
3.1.1.	Pressure loss in core region	3-1
3.1.2.	Natural convection in core and fuel assemblies	3-6
3.1.3.	Coolant mixing effect in upper plenum	3-9
3.1.4.	Heat transfer between tube and air of IRACS	3-21
3.2.	Integral Effects Tests	3-30
3.2.1.	Natural circulation in primary heat transport system	3-31
4.	CONCLUSION	4-1
5.	REFERENCES	5-1

LIST OF TABLES

Table No.	Title	Page No.
Table 2-1	Target events	2-1
Table 2-2	Selected phenomena for validation	2-3
Table 3-1	The Test Cases and Dimensionless numbers	3-4
Table 3-2	Test Results	3-5
Table 3-3	Test and analysis conditions	3-11
Table 3-4	Sodium Test Facility Specification Table	3-22
Table 3-5	Test condition	3-25
Table 3-6	Test Results	3-26
Table 3-7	Comparison between 4S and EBR-II [15, 16]	3-32
Table 4-1	Validation Results	4-1

LIST OF FIGURES

Figure No.	Title	Page No.
Figure 1-1	Schematic drawing of 4S facility	1-2
Figure 1-2	Heat transport system flow diagram	1-2
Figure 1-3	SAEMKON model	1-3
Figure 2-1	Validation target	2-2
Figure 2-2	Diagram of validation phases	2-5
Figure 3-1	Buoyancy effects on temperature peaking and friction factors [6]	3-2
Figure 3-2	Re Number Changes in the Reactor Core during LOSP	3-3
Figure 3-3	Gr Number Changes in the Reactor Core during LOSP	3-3
Figure 3-4	Gr/Re Changes in the Reactor Core during LOSP	3-4
Figure 3-5	SAEMKON afnalysis results	3-5
Figure 3-6	SAEMKON reactor core model	3-7
Figure 3-7	SAEMKON radial heat transfer model of reactor core	3-7
Figure 3-8	Comparison of thermal conductivity normal and reduced to half	3-8
Figure 3-9	Upper core plenum	3-12
Figure 3-10	Hydraulic test device	3-13
Figure 3-11	Points to obtain test data	3-14
Figure 3-12	SAEMKON test model	3-15
Figure 3-13	Axial temperature distribution (Case1)	3-15
Figure 3-14	Axial temperature distribution (Case2)	3-16
Figure 3-15	Axial temperature distribution (Case3)	3-16
Figure 3-16	Temperature shift (Case1)	3-17
Figure 3-17	Temperature shift (Case2)	3-17
Figure 3-18	Temperature shift (Case3)	3-18
Figure 3-19	Comparison of hydraulic head pressure (Case 1)	3-18
Figure 3-20	Comparison of hydraulic head pressure (Case 2)	3-19
Figure 3-21	Comparison of hydraulic head pressure (Case 3)	3-19
Figure 3-22	Effects of Nodalization	3-20
Figure 3-23	Heat removal of AC during LOSP	3-21
Figure 3-24	Flow rate of ACS durign LOSP	3-21
Figure 3-25	Sodium test facility of Toshiba Corporation	3-22
Figure 3-26	Sodium Test Facility Outline Drawing	3-23
Figure 3-27	SAEMKON Sodium test facility model	3-24
Figure 3-28	Heat transfer coefficient of test and SAEMKON	3-26

LIST OF FIGURES (cont.)

Figure No.	Title	Page No.
Figure 3-29	Comparison of SAEKMON and the test	3-27
Figure 3-30	Compensation coefficient including the scope of the test	3-28
Figure 3-31	Sodium temperature at ACS inlet/outlet during LOSP	3-28
Figure 3-32	Sodium temperature at core inlet/outlet during LOSP	3-29
Figure 3-33	Air temperature at ACS inlet/outlet during LOSP	3-29
Figure 3-34	XX09 subassembly[12]	3-33
Figure 3-35	Flow network model of EBR-II in SAEMKON	3-34
Figure 3-36	Comparison of coolant flow rate	3-35
Figure 3-37	Comparison of coolant temperature (TTC).....	3-36
Figure 3-38	Comparison of coolant temperature (MTC).....	3-36
Figure 3-39	Comparison of coolant temperature (14TC).....	3-37

LIST OF ACRONYMS AND ABBREVIATIONS

4S	Super-Safe, Small and Simple
AC, ACS	Air Cooler, Air Cooler System
ANL	Argonne National Laboratory
AOO	Anticipated Operational Occurrence
ATWS	Anticipated Transients Without Scram
BDBA	Beyond-Design-Basis Accident
BOP	Balance of Plant
CDF	Cumulative Damage Fraction
CFD	Computational Fluid Dynamics
CRIEPI	Central Research Institute of Electric Power Industry
DA	Design Approval
DBA	Design Basis Accident
DBE	Design Basis Event
DRACS	Direct Reactor Auxiliary Cooling System
EBR	Experimental Breeder Reactor
EMF	ElectroMagnetic Flowmeter
EMP	ElectroMagnetic Pump
FCC	Failure of a Cavity Can
FP	Fission Product
FR	Fast Reactor
GV	Guard Vessel
H, M, L	High, Medium, Low
I&C	Instrumentation and Control
IC	Inner Core
IET	Integral Effects Test
IHX	Intermediate Heat exchanger
IHTS	Intermediate Heat Transport System
IRACS	Intermediate Reactor Auxiliary Cooling System
ISI	In-Service Inspection
K, P, U	Known, Partially known, Unknown
LOCA	Loss of Coolant Accident
LOF	Loss of Flow
LOSP	Loss of OffSite Power
LMR	Liquid Metal Reactor
LWR	Light Water Reactor

MC	Middle Core
MG	Motor Generator
NRC	Nuclear Regulatory Commission
OC	Outer Core
PCT	Peak Cladding Temperature
PHTS	Primary Heat Transport System
PIRT	Phenomena Identification and Ranking Table
RHRS	Residual Heat Removal System
RV	Reactor Vessel
RVACS	Reactor Vessel Auxiliary Cooling System
S/A	SubAssembly
SAEMKON	Safety Analysis for Energy, Motion, Kinetics, One dimensional Flow-Network
SET	Separate Effects Test
SG	Steam Generator
SLIP	Sodium Leakage from Intermediate Piping
SoK	State of Knowledge
SR	Shutdown Rod
SRP	Standard Review Plan

Abstract

Toshiba Corporation (Toshiba) is planning to apply for licensing of the Super-Safe, Small and Simple (4S) reactor in the United States with the cooperation of the Central Research Institute of Electric Power Industry (CRIEPI), Westinghouse Electric Company, and Argonne National Laboratory (ANL). Toshiba, supported by the aforementioned parties, have held pre-application review meetings with the U.S. Nuclear Regulatory Commission (NRC) in preparation for licensing.

This document provides a description of the SAEMKON validation for loss of offsite power event. SAEMKON is a TOSHIBA safety analysis code, developed in-house, and a kind of one-dimensional flow network code. This report is corresponding to the technical report of "Plant Dynamics Analysis Code" which is listed in "Schedule for 4S Technical Reports Submittal" (ADAMS No. ML110820191, Table 1). According to NUREG-1737 "Software Quality Assurance Procedures for NRC Thermal Hydraulic Codes", the elements of software quality assurance is classified to 6 life cycle [4, Chapter 3, Table 1], and this report is corresponding to the software testing phase.

The 4S system design of the 30MWt version is completed and the licensing activities have commenced. In licensing activities, safety analyses are performed by using SAEMKON. To satisfy the U.S. Nuclear Regulatory, the code verification and validation (V&V) should be performed.

In verification, the equation and coding have been verified through line by line check. In validation, the capability to evaluate particular events has been validated. Among the transient events, Loss of Offsite Power Event (LOSP) is selected as one of the example for validation in this paper. The code assessment procedure can be classified 3 phases, Separate Effects Test (SET) phase, Integral Effects Test (IET) phase and Applicability Demonstration phase (confirm that SAEMKON has the capability of analyze particular event). The former two phases, SET and IET, is the code validation phases.

In SET phase, the analysis results of the important phenomena should be evaluated with using theoretical solutions, other validated computer programs, experimental results, standard problems with known solutions, or published data and correlations. The important phenomena of LOSP are selected by PIRT (Phenomena Identification and Ranking Tables) and the phenomena are classified into 5 types. To validate the code with 5 types of phenomena, various evaluations have been performed.

In IET phase, the test data of EBR-II (Experimental Breeder Reactor-II) are used and the capability of the code to simulate natural circulation behavior of the plant is confirmed.

In this paper, these validation results of the 4S safety analysis code for LOSP are described.

1. INTRODUCTION

1.1. 4S Plant Design

Toshiba Corporation and CRIEPI (Central Research Institute of Electric Power Industry) have jointly developed the Super-Safe, Small and Simple (4S) sodium-cooled reactor (Figure 1-1) [1]. Since the 4S design is intended for application to a site in areas without a well-developed grid, like an isolated area in Alaska in the U.S., features of the reactor design include no refueling for 30 years to reduce the burden of fuel transportation to these remote areas, and passive safety features reduce the demands on the operator's support.

A pool type fast neutron reactor, the 4S, has a primary electrical output of 10MWe (30MWt). Figure 1-1 shows a schematic drawing of the overall 4S based on power generation facility depicting its major components. The reactor vessel is located below grade, and includes the intermediate heat exchanger (IHX), electromagnetic pumps (EMPs), internal structures, core and shielding, and containment system (consisting of the top dome and guard vessel). The primary heat transport system is enclosed within the reactor vessel. Figure 1-2 shows the heat transport system flow diagram. Heat from the single loop of the intermediate heat transport system (IHTS) is exchanged in a steam generator (also located below grade) to produce steam.

The system design of the 30MWt version is completed and the licensing activities have commenced. In licensing activities, safety analyses using TOSHIBA self-developed safety analysis code "Safety Analysis for Energy, Motion, Kinetics, One dimensional Flow-Network (SAEMKON)" have been planned.

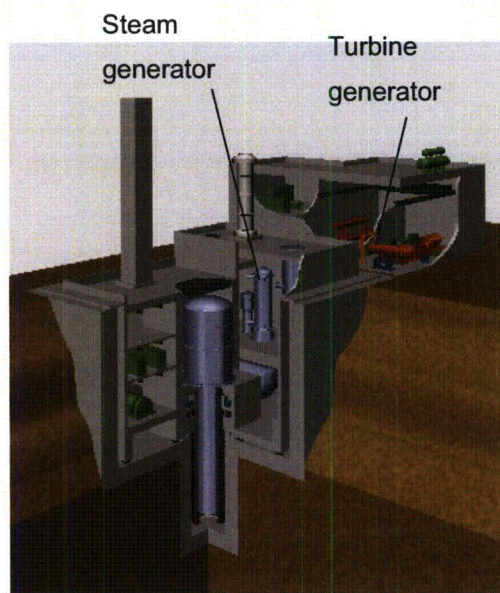


Figure 1-1 Schematic drawing of 4S facility

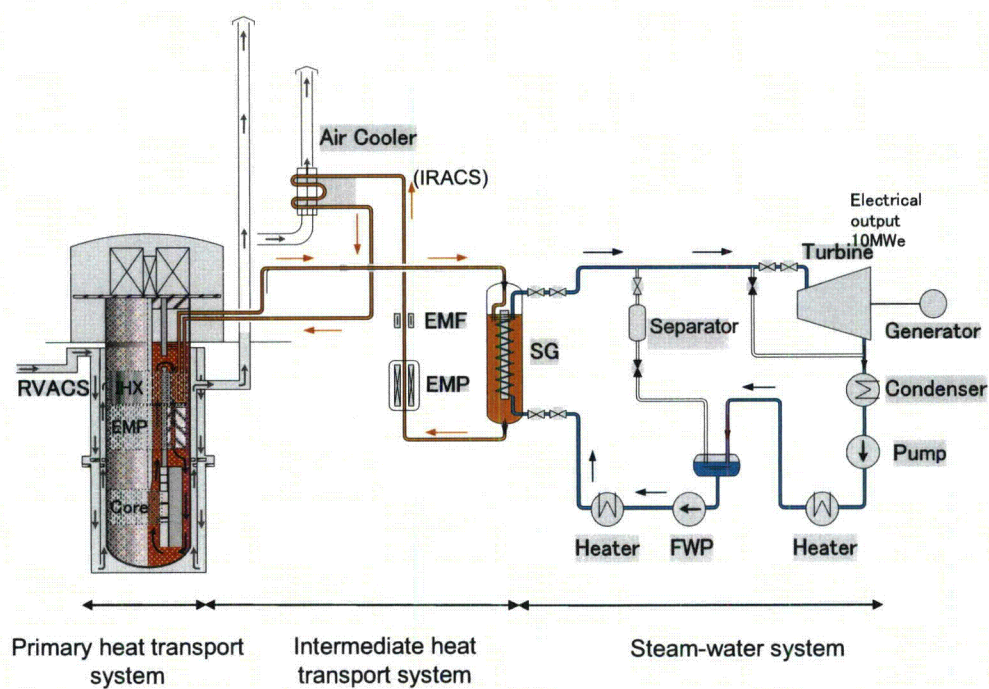


Figure 1-2 Heat transport system flow diagram

1.2. Safety Analysis Code SAEMKON

SAEMKON is the TOSHIBA self-developed safety analysis code and it is a one dimensional flow network code (Figure 1-3). SAEMKON models 4S plant from the reactor core to steam generator (SG). The reactor core consists of core element such as Shutdown rod, Inner core, Middle core, Outer core, and reflector.

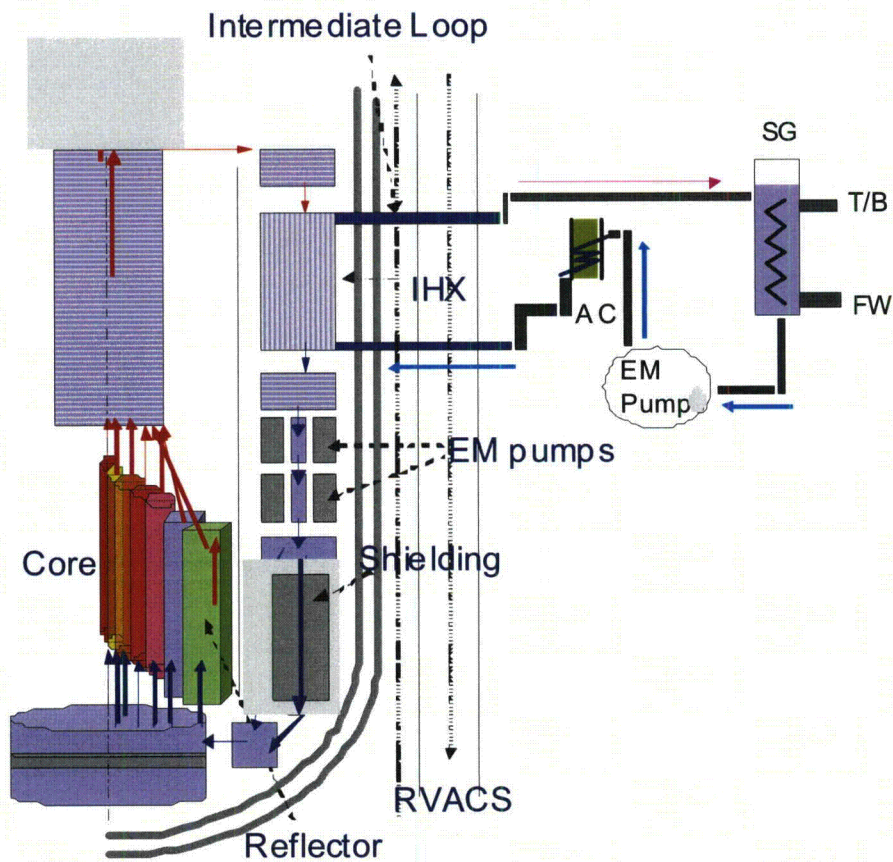


Figure 1-3 SAEMKON model

The objective of the analysis using the SAEMKON is to evaluate the integrity of fuel pins and the temperature of the primary coolant boundary during DBEs (Design Basis Events) and beyond-DBEs such as ATWS (Anticipated Transients Without Scram). The main design basis events to be considered are an increase or decrease in heat removal by the balance of plant (BOP), decrease or increase of flow in the primary- or intermediate-loop coolant, an anticipated reactivity insertion at full-power operation or startup, and loss of electrical power. Regarding these events, to calculate fuel cladding temperature and primary coolant boundary temperature with sufficient precision, the plant transient states must be modeled correctly.

The SAEMKON models the movement of a one dimensional incompressible fluid, and expresses the fluid flow according to the one dimensional flow network model, including the intermediate heat exchanger, the steam generator and the core, and starting from an initial steady thermal-hydraulic balance, analyzes the transient.

The core is modeled with multiple parallel channels, with each channel representing one pin enclosed in the associated wrapper duct. The one dimensional flow in the channel absorbs heat from the fuel pins and flows out from the channel; the flow of each channel joins at the channel exit. The fuel, cladding, and coolant in the core are divided in the axial direction. The fuel pellet or slug is further divided in the radial direction into cells.

Nuclear dynamic characteristics (kinetics) are calculated as the reactor power transient with a one-point approximation model (point kinetics) and six group delayed neutron precursors. The reactivity contributions include the insertion reactivity, scram reactivity, Doppler feedback, and a reactivity feedback by the temperature change of the fuel, cladding, and wrapper duct.

During the rated operation, the coolant flows around the wrapper tube with a wide gap which resistance of the pressure loss is small. On the other hand, during the reactor trip, the coolant unevenly flows into the center of hot fuel assemblies because the drive is switched to natural circulation. The pressure loss of the fuel assemblies increases because the coolant unevenly flows into the region with a narrower gap. SAEMKON models the phenomenon of increasing pressure loss with test data of reference material [6].

The SAEMKON models the equation of motion of the fluid in the one dimension by balancing the pump head, natural convection head, and pressure loss. The friction pressure loss is expressed in a form depending on the Reynolds Number and shape pressure loss is included. The motion equation of the flow network is systematically solved by considering the flow distribution in the reactor core, flow of the heat transport system, and flow in the heat exchanger.

Heat transfer by forced convection, natural convection, and radiation can be modeled. Such

heat transfer is selected from a choice of forced convection, natural convection, radiation, or the constant type. In other words, the radiation heat transfers from RV (Reactor Vessel) to GV (Guard Vessel) and from GV to collector, the convective heat transfer from GV to air and from collector to air, and the air motion (i.e., the process in which the air takes in the atmospheric air, receives the released heat, rises due to natural circulation head, and is dissipated into the atmospheric air) are all described.

This code models general events and interlocks such as the initiator and scram signal, e.g., a pump trip, scram, and flow path failure (leakage and opening or closing of a valve) during a transition.

The transient trigger is expressed by the general interlock model: namely, pump trip, scram, occurrence and the loss of flow path, opening and closing of the valve, etc., actuated by a general signal that is, in other words, the specified delayed time in the event that the temperature, pressure, fluid level, head, flow rate, etc., decrease below or increase above the specified set point.

2. VALIDATION STRATEGY

2.1. Events Selection

The selected events in technical report “4S Safety analysis” are shown in Table 2-1[2]. The validation target events of SAEMKON are selected from this table considering inclusiveness.

Table 2-1 Target events

	Safety analysis events
AOO	Loss of Offsite Power
	Decrease of Primary Coolant Flow
	Reactivity Insertion by Uncontrolled Motion of Segments Reflector at Startup
	Inner or Outer Tube Failure of Steam Generator
	Failure of a Cavity Can
DBA	Sodium Leakage from Intermediate Piping
	Loss of Offsite Power without Scram
ATWS	

AOO: Anticipated Operational Occurrence

DBA: Design Basis Accident

ATWS:Anticipated Transients without Scram

Among the events, Loss of Offsite Power Event (LOSP) is selected as one of the example for validation in this paper. This event involves transmission system failure or offsite power electrical equipment failure during reactor rated operation. After the loss of power supply for the station, primary flow and intermediate flow are gradually decreased and reach to natural circulation flow. The residual heat is removed by the reactor vessel auxiliary cooling system (RVACS) and intermediate reactor auxiliary cooling system (IRACS) by natural circulation [2].

2.2. Target Phenomena

The Validation target phenomena of LOSP are selected by PIRT (Phenomena Identification and Ranking Tables)[3]. The PIRT classify phenomena into 9 types with importance and state of knowledge as shown in Figure 2-1. The patched area is the target of validation. The selected phenomena are classified into 5 types as shown in Table 2-2. To validate the code with 5 types of phenomena, varied evaluation has been performed.

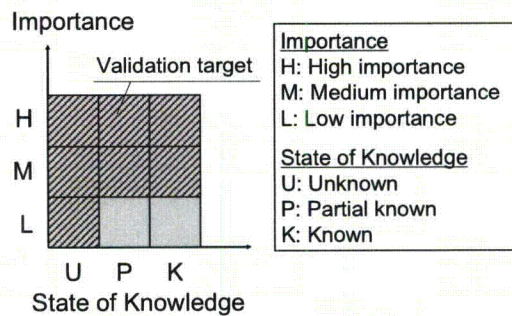


Figure 2-1 Validation target

Table 2-2 Selected phenomena for validation

No.	Selected Phenomena	Importance and state of knowledge	Validation target	Validation Type
1	Pressure loss in fuel assembly	M-P	(1) Local pressure loss in core region derive from inter-assembly flow distribution	Separate Effect Test
2	Intra- and inter-assembly flow distribution	H-P		
3	Maldistribution of the core flow: redistribution of the mass flow in all core subassemblies	H-P	Set aside from validation target	
4	Inter-wrapper flow between wrapper tubes	M-P		
5	Natural convection in core region	M-P	(2) Global phenomena in core region derive from three dimensional flow	
6	Radial heat transfer from and to subassemblies and sodium	M-P		
7	Coolant mixing effect in upper plenum including thermal stratification	M-P	(3) Coolant mixing effect in upper plenum (thermal stratification)	
8	Heat transfer of IRACS between tube and air	M-P	(4) Heat transfer of IRACS between tube and air	
9	Inlet air temperature range	M-K	Set aside from validation target	
10	Natural convection in reactor system	M-P	Included in (2) and (3)	Integral Effect Test & Applicability Demonstration
11	Natural circulation in primary heat transport system	M-P	(5) Global transient behavior of full scale plant in Natural convection and circulation phase	
12	Natural circulation in intermediate heat transport system	M-P	Included in Applicability demonstration phase	

There are four phenomena related to core; "Pressure loss in core region", "Intra- and inter-assembly flow distribution", "Maldistribution of the core flow" and "Natural convection in core region" (No. 1, 2, 3, 5). The first three phenomena are local phenomena due to fuel assemblies and No. 5 is an overall phenomenon due to the distribution of the assemblies. No. 3 is caused by the difference in the production process so validation is not required. If the increasing effect of the pressure loss caused by Maldistribution needs to be included in SAEMKON based on the design review, the sensitivity of "Maldistribution of the core flow" is verified. Also, regarding No. 4, the Inter-assembly area is shut by pad and Inter- assembly flow distribution is sufficiently small so validation is not required. The major phenomenon of Pressure loss in core region is inter- assembly flow distribution. Thus, regarding the local core pressure loss, the validation is required for intra-assembly flow distribution.

Regarding No.5 and No.6, the point of these phenomena is radial heat transfer of core region. Since the 4S inter-wrapper region is closed by pad and the flow rate among assemblies is small, inter-wrapper flow has a small effect on the heat transfer between wrapper tube wall and coolant. In addition, sodium transfer the heat by rather conduction than convection and heat conduction coefficient of SAEMKON is set conservatively. The effect of radial heat transfer is discussed in Chapter 3.1.2.

Regarding No.9, the ambient air temperature is not sort of validation item, and this phenomena is set aside from validation target.

"Natural convection in reactor system", No.2, is evaluated as a significant phenomenon in Chapter 3.1.2 "Natural convection in core region" and Chapter 3.1.3 "Coolant mixing effect in upper plenum". These two phenomena are independent phenomena in this LOSP event. Thus, regarding No. 10 "Natural convection in reactor system", it is included in Chapter 3.1.2 and Chapter 3.1.3.

No.12 "Natural circulation in intermediate heat transport system" is included in Applicability Demonstration.

2.3. Test Type

The code assessment procedure can be classified 3 phases, Separate Effects Test (SET) phase, Integral Effects Test (IET) phase and Applicability Demonstration phase (confirm that SAEMKON has the capability of analyze particular event). The former two phases, SET and IET, is the code validation phases. The conceptual images of each phase are shown in Figure 2-2. The safety report requires some analysis of representative events for SAEMKON as shown in Table 2-1. Each event has important phenomena which is selected by PIRT respectively. The concept of SET is to compare the important phenomenon with reference data such as test data, published data, etc. The concept of IET is to compare the effects of complicated phenomena with plant scale data. The concept of Applicability Demonstration is to evaluate the capability of analysis for the representative event.

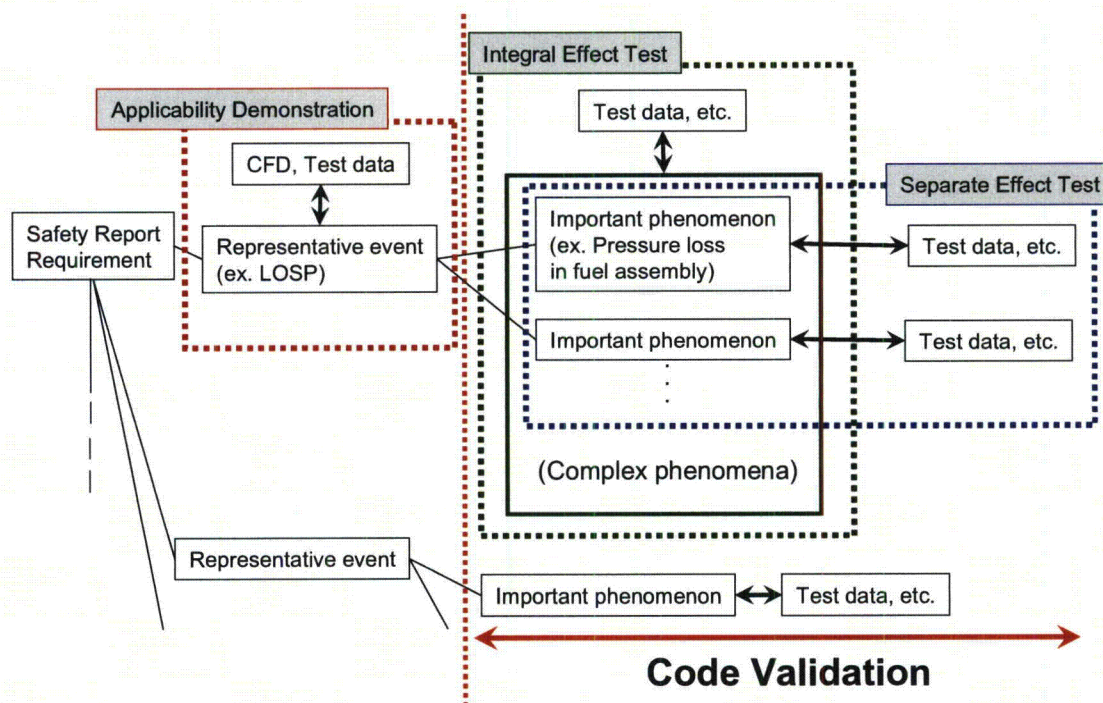


Figure 2-2 Diagram of validation phases

The details of each phase are the followings.

(1) Separate Effects Test

In SET phase, the analysis results of the important phenomena should be evaluated with

using theoretical solutions, other validated computer programs, experimental results, standard problems with known solutions, or published data and correlations[4]. The tests include the followings;

- Water hydraulic test
- Data of sodium test facility
- Published data

(2) Integral Effects Test

In IET phase, the test data of EBR-II are used and the capability of the code to simulate natural circulation behavior of the plant is confirmed. The tests include the followings;

- EBR-II Shutdown Heat Removal Test

2.4. Acceptance Criteria

The safety criteria for the safety analysis of the 4S reactor are defined as follows, considering the guidance of SRP 15.0 (Standard Review Plan) [5], and making allowance for differences between LMRs and LWRs [2].

1. Safety criteria for AOOs
 - Maintaining the fuel cladding integrity
 - Maintaining the primary coolant boundary integrity
2. Safety criteria for DBAs
 - Maintaining the core coolable geometry
 - Maintaining the primary coolant boundary integrity
 - Maintaining the allowable radiation exposure at an exclusion area boundary
3. Safety criteria for ATWS
 - Maintaining the core coolable geometry
 - Maintaining the primary coolant boundary integrity
 - Maintaining containment integrity

Most of these criteria, which should be evaluated by SAEMKON, is concerned about evaluation of core damage. From the view point of code validation, these criteria are integrated into Cumulative Damage Fraction (CDF) of fuel. To evaluate boundary integrity, SAEMKON is required to simulate temperature distribution and flow rate correctly. The core inlet temperature is uniform because the heat capacity of radiation shield is high. The IHX inlet temperature is depend on the core outlet temperature and mixing effect of core upper plenum. The mixing effect of core upper plenum and plant scale natural circulation is evaluated as shown in Chapter 3.1.3 and 3.2 of this report. So, the SAEMKON's criteria come down to maximum temperature of fuel cladding. If the evaluating model is not including the calculation of cladding temperature, equivalent parameters such as core outlet temperature, primary flow rate, and heat removal are evaluated.

Each validation qualitative acceptable criteria is mainly based on NUREG-1737 Appendix C[4]. In qualitative assessment the conclusions are based on user's judgment and experience.

(1) Good agreement

“Good agreement” applies when major phenomena and trends are correctly predicted. The term “major phenomena” refers to phenomena that influence key parameters for fuel cladding temperature, such as temperature, pressure, flow rate, and mass distribution. Predicting the major trends means that the prediction shows the significant features of the data.

(2) Reasonable agreement

“Reasonable agreement” applies when the trends exhibit minor difference between calculated values and data. Overall, the code provides an acceptable prediction and the correct conclusions about trends and phenomena would be reached if the code was used in similar applications.

(3) Insufficient agreement

“Insufficient agreement” applies when the code does not satisfy above criteria. The code should be reviewed and modified.

3. VALIDATION RESULTS

3.1. Separate Effects Tests

3.1.1. Pressure loss in core region

(1) Phenomena description and validation objective

The validation point of this phenomenon is that, under the natural circulation during transient, the flow redistribution occurs due to buoyancy effect in subassembly and causes the increase of the pressure drop of a bundle. During the rated operation, the flow distribution in fuel subassembly, the flow rate of inner sub-channel is approx. 10% smaller than the average flow rate. So the fuel pin temperature is higher than the average flow channel. After reactor trip, the flow rate of hot sub-channel increases and the flattening of temperature distribution occurs in fuel subassembly. This phenomena increase the pressure loss coefficient in the fuel assemblies. In the fuel assemblies, there are 169 fuel pins and they are wound by the wire.

The coolant from the entrance nozzle flows around the fuel pins and flows from the handling head to the upper plenum. During the process, the coolant flows through the fuel cladding so that the temperature rises due to the heat from the fuel. During the rated operation, more coolant flows around the wrapper tube than center due to the pressure loss is small. On the other hand, after the reactor trip, the coolant unevenly flows into the center of hot fuel assemblies because the drive is switched to natural convection. The pressure loss of the fuel assemblies increases because the coolant flow rate of the region in narrower gap increases.

In this Separate Effect Test, the phenomenon of the increasing pressure loss coefficient during natural convection is validated.

According to the reference [6], in order to contribute to the soundness of the fuel during the operation to remove decay heat by natural convection, the relation of the temperature distribution in the pin bundle cross dimension and the flow resistance from natural convection to forced convection region are examined by the sodium test with 37 pin bundles and the water flow test with 91 pin bundles. As a result of those tests, the similar trend is identified in both the sodium test and the water flow test. And then, it is identified that the peaking coefficient of the diameter direction temperature under natural convection, mixed convection and forced convection can be described by using $Gr_{\Delta T}/Re_D$. Also, from the relation between the temperature peaking and friction loss of the pin bundles, it is identified that the increasing friction loss is caused by the redistribution of the flow. The relation of $Gr_{\Delta T}/Re_D$, peaking coefficient and pressure loss coefficient is shown as Figure 3-1 and that shows the trend mentioned above.

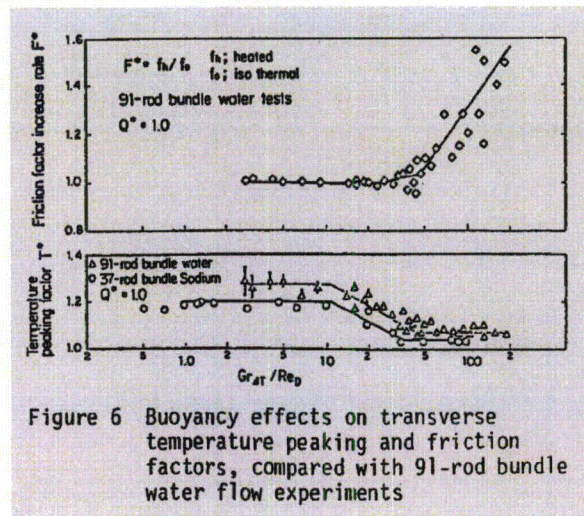


Figure 3-1 Buoyancy effects on temperature peaking and friction factors [6]

(2) Test plan

In these tests, by using the core fuel model of SEAMKON, the increasing coefficient of core pressure loss in case natural convection becomes more significant than forced convection and the increasing ratio are compared with the reference[6]. In 4S, the peaking coefficient during the natural convection uses the same value during the rated operation. Thus, the result becomes conservative.

In these tests, $Gr_{\Delta T}/Re_D$ becomes dimensionless parameters as shown in the reference [6].

$$Gr_{\Delta T} = \frac{g\beta(T_o - T_i)D_h^3}{\nu^2}$$

$$Re_D = \frac{(UD_h)}{\nu}$$

$Gr_{\Delta T}$: Grashof number

Re_D : Reynolds number

g : Acceleration of gravity

β : Expansion rate

U : Flow rate

ν : dynamic viscosity

T_o : Bulk assembly temperature of outlet

T_i : Bulk assembly temperature of inlet

D_h : Hydraulic diameter (Diameter of assembly)

Figure 3-2 through Figure 3-4 show changes in dimensionless numbers during LOSP.

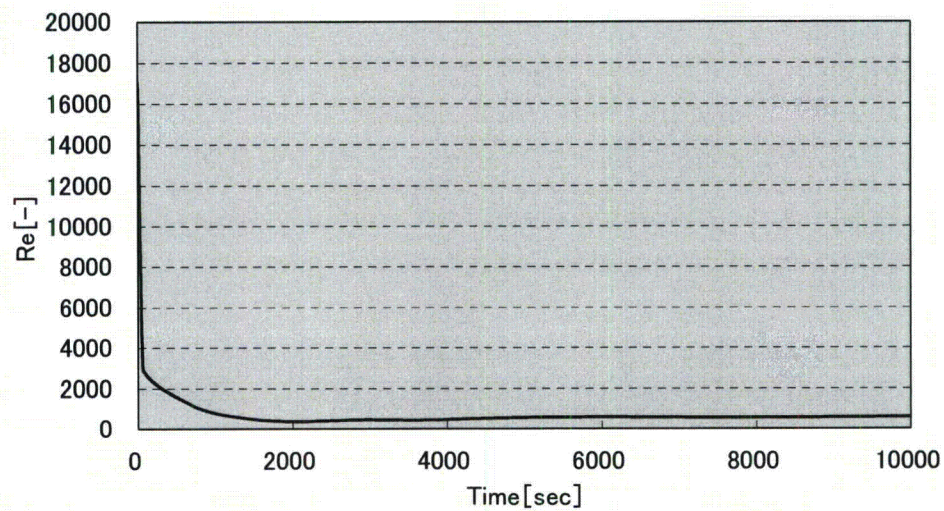


Figure 3-2 Re Number Changes in the Reactor Core during LOSP

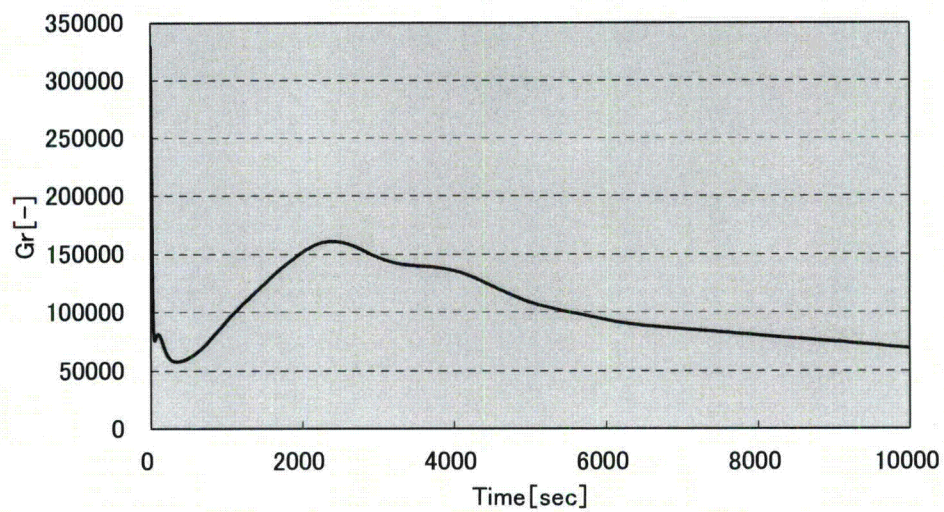


Figure 3-3 Gr Number Changes in the Reactor Core during LOSP

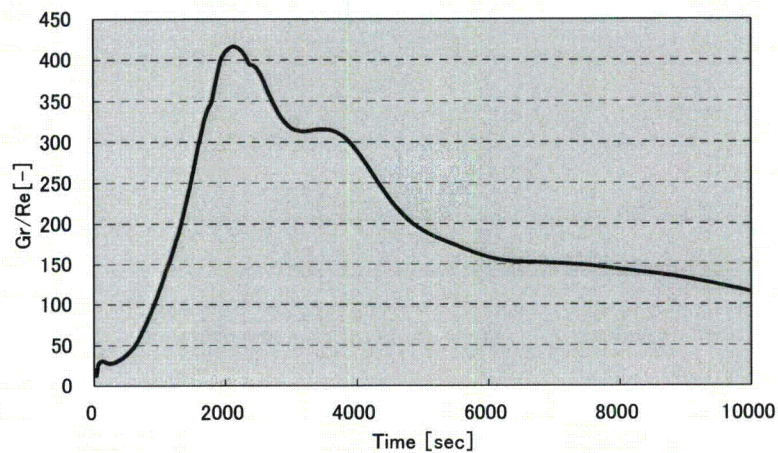


Figure 3-4 Gr/Re Changes in the Reactor Core during LOSP

Considering maximum and minimum values of Gr/Re and inflection point(s) obtained from references during LOSP, the test case is set up as shown in Table 3-1.

The test cases of the dimensionless figures are also shown in this table.

Table 3-1 The Test Cases and Dimensionless numbers

	4S $Gr_{\Delta T}$	4S Re_D	$Gr_{\Delta T}/Re_D$	F
Test Case1	3.30×10^5	1.66×10^4	19.9	1.00
Test Case2	6.65×10^4	1.33×10^4	50.1	1.04
Test Case3	8.63×10^4	8.62×10^2	100	1.30
Test Case4	1.13×10^4	5.75×10^2	196	1.54

"F" shows Friction factor in Figure 3-1.

(3) Test result

The analysis results are shown in Figure 3-5 and these data are compared with reference data in Table 3-2.

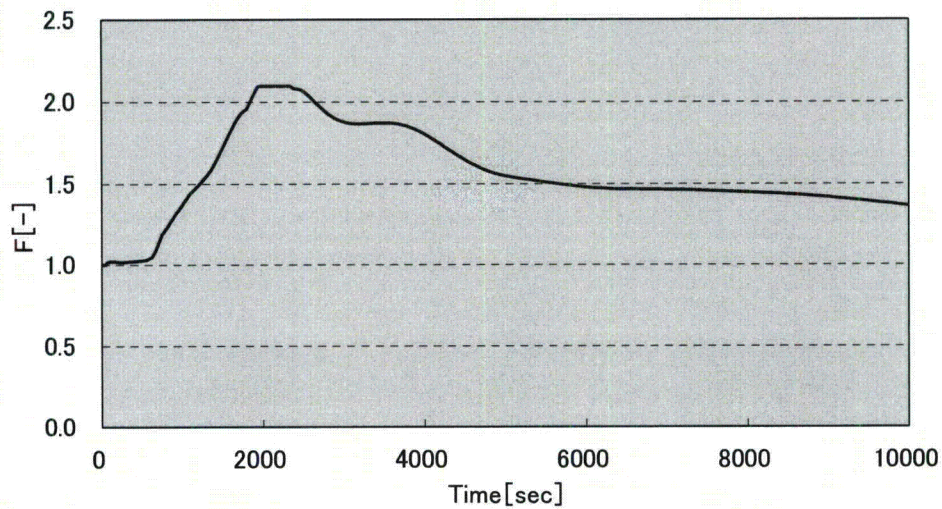


Figure 3-5 SAEMKON afnalysis results

Table 3-2 Test Results

	4S Gr _{ΔT}	4S Re _D	Gr _{ΔT} /Re _D	F	Analysis results
Test Case1	3.30x10 ⁵	1.66 x10 ⁴	19.9	1.00	1.00
Test Case2	6.65 x10 ⁴	1.33 x10 ⁴	50.1	1.04	1.05
Test Case3	8.63 x10 ⁴	8.62 x10 ²	100	1.30	1.32
Test Case4	1.13 x10 ⁴	5.75 x10 ²	196	1.54	1.56

The results show that F values correspond with the analysis results.

(4) Consideration

Above the result, SAEMKON results well correspond to Test data and are evaluate as a good agreement.

3.1.2. Natural convection in core and fuel assemblies

(1) Phenomena description and validation objective

The point of this phenomenon is redistribution in core region. During rated operation, the flow is driven by pumps and flow distribution depends on pressure loss in fuel assemblies. After switched to natural convection, the flow is driven by natural convection force and flow distribution depends on temperature distribution and pressure loss in fuel assemblies. So, to evaluate the phenomenon of redistribution correctly, radial heat transfer and pressure loss in core region are important parameter. The pressure loss in core region is evaluated in Chapter 3.1.1. In this chapter, the effect of radial heat transfer is discussed.

(2) Test plan

In the reference [7,8,9], the effect of radial heat transfer for core outlet temperature is discussed with same type of flow network model to SAEMKON as shown in Figure 3-6 and Figure 3-7. According to these references, to model the radial heat transfer makes the results more accurate. It is also mentioned that omitting radial heat transfer model makes the inner core outlet temperature higher because the radial temperature distribution around fuel assemblies will not be uniform. In this chapter, the parametric analysis of thermal conductivity is performed.

(3) Test result

Figure 3-8 shows the comparison of thermal conductivity normal and reduced to half. In the reference [9], to model the radial heat transfer makes the maximum temperature low and this result shows same inclining with this reference. So, it is confirmed that the intendency of SAEMKON correspond qualitatively to the reference. The quantitative evaluation is performed in Chapter 3.2 with using EBR-II model and it is confirmed that the core outlet temperature of SAMEKON is correspond to the test result.

(4) Consideration

It is also reported in reference [9] that the sensitiveness of heat transfer coefficient is low for core outlet temperature. Thus this model is evaluated as good agreement.

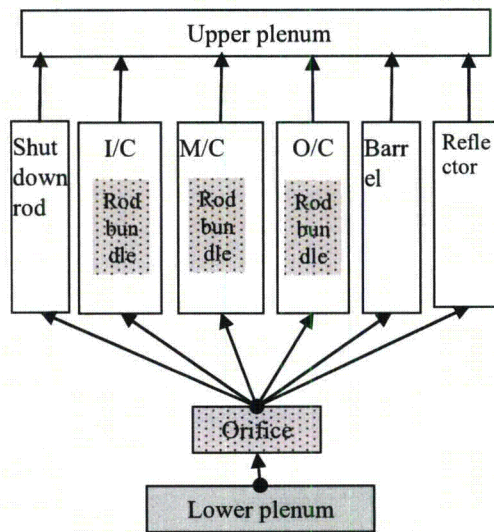


Figure 3-6 SAEMKON reactor core model

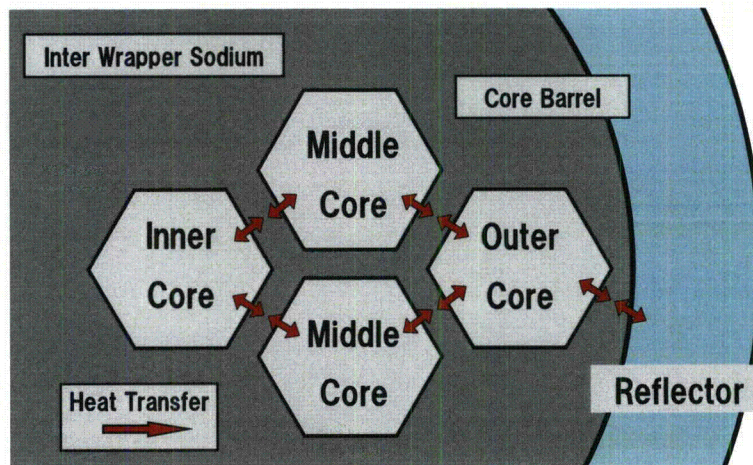


Figure 3-7 SAEMKON radial heat transfer model of reactor core

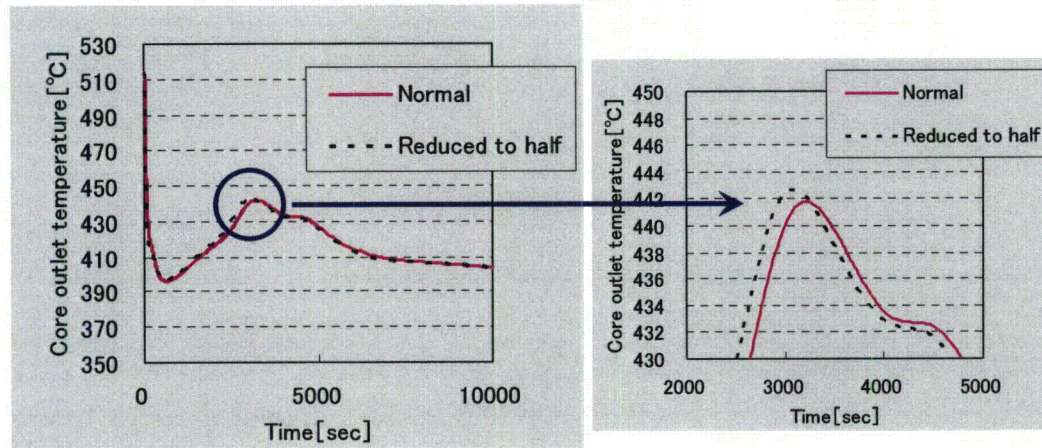


Figure 3-8 Comparison of thermal conductivity normal and reduced to half

3.1.3. Coolant mixing effect in upper plenum

(1) Phenomena description and validation objective

The validation of the upper core plenum region during a LOSP event is discussed in this chapter.

The outline drawing of the upper core plenum in 4S is shown as Figure 3-9. The upper core plenum in 4S is shaped as a tall cylinder and the upper core structure is placed at its center. Also, a vertical partition exists in an outer wall of the plenum and the coolant flows into an IHX (Intermediate Heat Exchanger), climbing through the top of the vertical partition.

In the LOSP event, since low-temperature coolant flows from the core region into the upper plenum where the high-temperature coolant remains, there is a possibility of causing thermal stratification. The thermal stratification may affect natural circulation in the reactor vessel.

Stratification occurs due to the balance between fluid buoyancy and inertial force in the upper core plenum. Thus, the scope of examination was specified by using Richardson number (Ri) as defined in the following formula. The range of Ri number is from 4500 to 72000 in the 4S during LOSP so that validation including the range is required.[10]

$$Ri = \frac{\beta g \Delta T l^+}{u^{+2}}$$

u^+ : Characteristic velocity

(mean flow velocity of the plenum)

l^+ : Characteristic distance

(hydraulic equivalent diameter of the plenum)

g : Acceleration of gravity

β : Thermal expansion coefficient

ΔT : Temperature difference

(2) Test plan

SAEMKON for this phenomenon was validated by comparing with the result from the hydraulic test. The small-sized apparatus with 1/3 scale and 60 degree sector was used in the hydraulic test. The apparatus are shown in Figure 3-10 and Figure 3-11. The simulation of LOSP in the upper core plenum was conducted based on the following procedures:

1. Specify fluid temperature and flow rate as test conditions to achieve the Ri number that corresponds with the conditions of the 4S plant scale equipment.
2. Store hot water in the upper core plenum.
3. Flow cold water into the upper core plenum from a hole modeled as a core at fixed rate.
4. Obtain the data of transient temperature from the thermoelectric pile placed at the axial direction in the apparatus.

The test model of the upper core plenum in SAEMKON is shown as Figure 3-12. In this model, dimension of the plenum, fluid capacity and heat capacity of steel are the same as those in the test model. The number of nodalization in the plenum was 300. By using the model, the hydraulic head pressure in the plenum calculated by the axial temperature distribution was compared with the test result and the validation was conducted. In case 2, to simulate the temperature decreasing by heat release, the effect of heat release is modeled.

The hydraulic head pressure is a factor that effects on the core flow rate during the natural circulation of 4S and specified by the following formula;

$$\text{Hydraulic head pressure} = \int_{h_0}^{h_t} (\rho_{\text{initial}} - \rho_t(h)) \cdot g \cdot dh$$

h_0 : height of core outlet (bottom of upper plenum)

h_t : top of upper plenum cylinder (Figure 3-11, At 2.767 m from bottom)

$\rho_t(h)$: density at the time t

ρ_{initial} : initial density

Three cases shown as Table 3-3 were specified as test and analysis conditions.

(3) Test result

The comparison of axial temperature distribution is shown as Figure 3-13 through Figure 3-15. The vertical axis indicates height and the horizontal axis indicates temperature. According to the figure, in the range of Ri number during LOSP in 4S, all results show piston flow and the mixture of hot and cold water is rarely seen because fluid buoyancy is dominant. Also, the axial temperature distribution corresponds with the test well at each time period. The temperature shift of top of upper plenum cylinder are shown in Figure 3-16 through Figure 3-18. The time transient of hydraulic head pressure in the plenum is shown as Figure 3-19 through Figure 3-21. The vertical axis indicates hydraulic head pressure and the horizontal axis indicates time. According to the Figure, it is identified that the transient of hydraulic head pressure in SAEMKON corresponds well in any range of Ri number.

(4) Consideration

Based on the above results, in the range of Ri during LOSP in 4S, SAEMKON results are well corresponding to the hydraulic test results and it is evaluated as good agreement. Also, in the flow network code, nodalization may effect on the analysis result, the parameter analyses have been performed with changing the number of nodalization in the plenum region. The transition of hydraulic head pressure by the plenum division number is shown as Figure 3-22. As the division number increases, the hydraulic head pressure becomes close to the test result. Based on the result, it was determined that approximately 300 of division number is sufficient for the simulation of the test.

Table 3-3 Test and analysis conditions

	Test Case 1	Test Case 2	Test Case3
Flow rate [kg/sec]	0.332	0.0220	0.664
Initial Plenum Temperature [°C]	42.3	45.2	49.7
Influx Temperature [°C]	11.6	11.2	9.70
Ri number [-]	300	81000	100

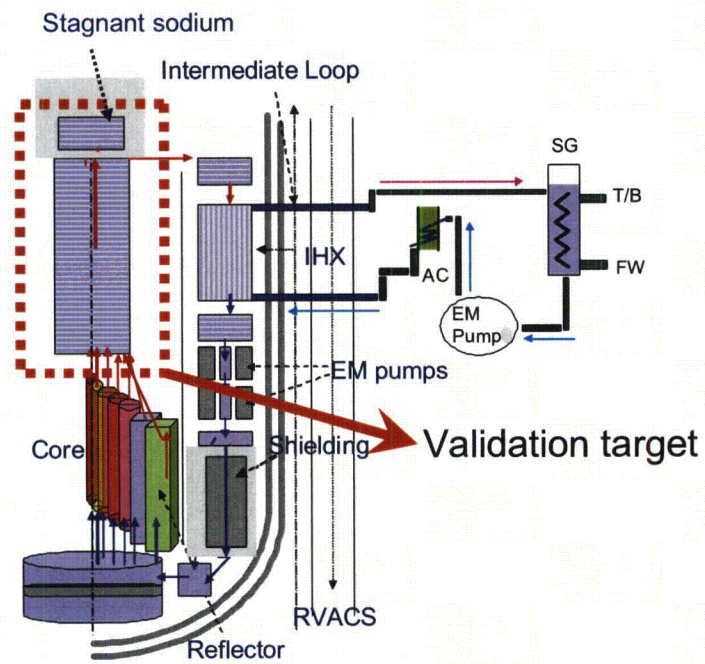


Figure 3-9 Upper core plenum

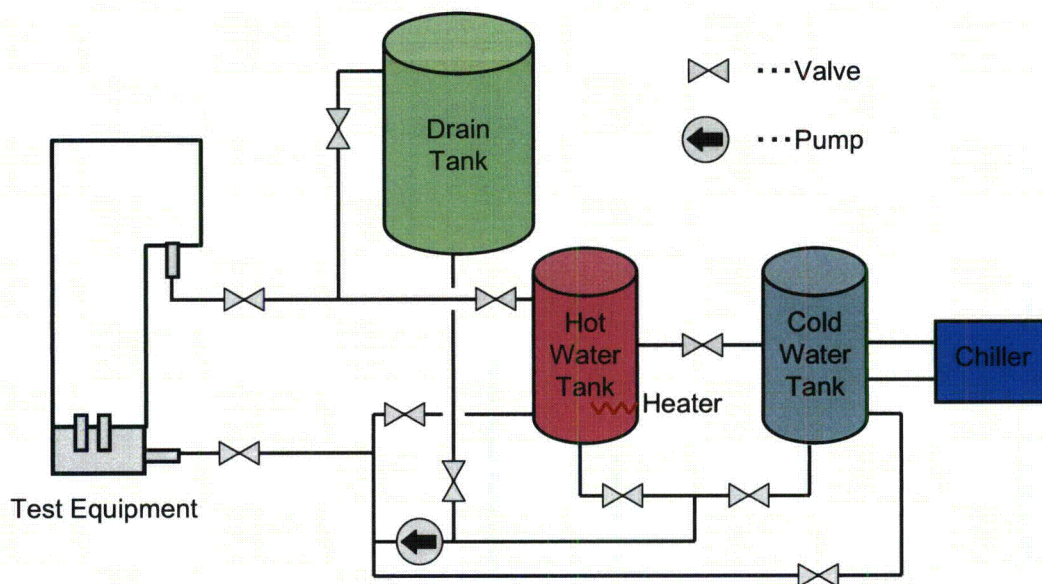
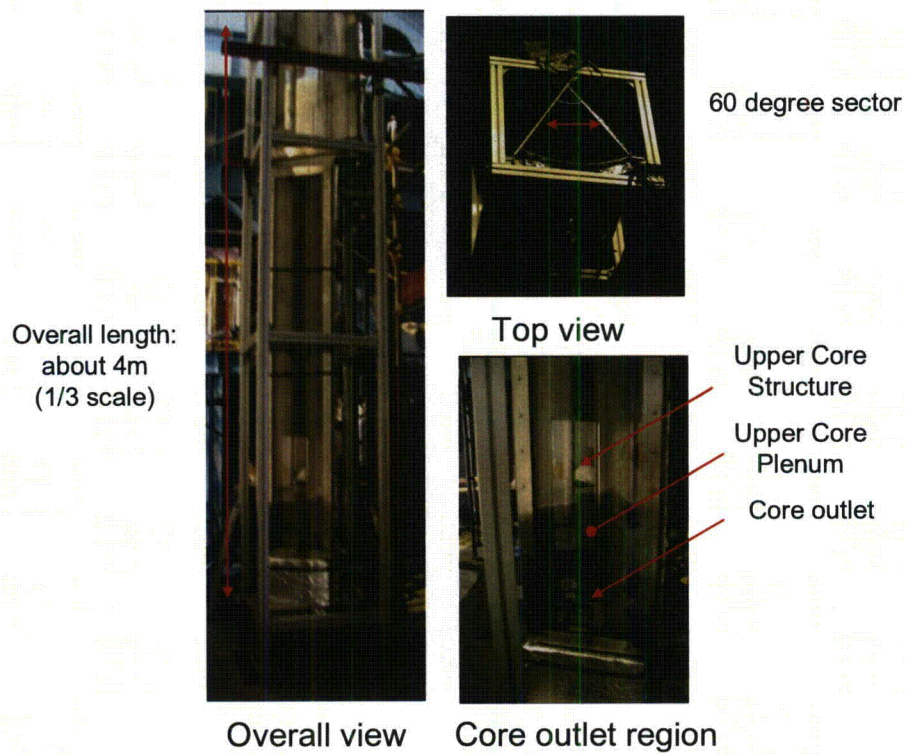


Figure 3-10 Hydraulic test device

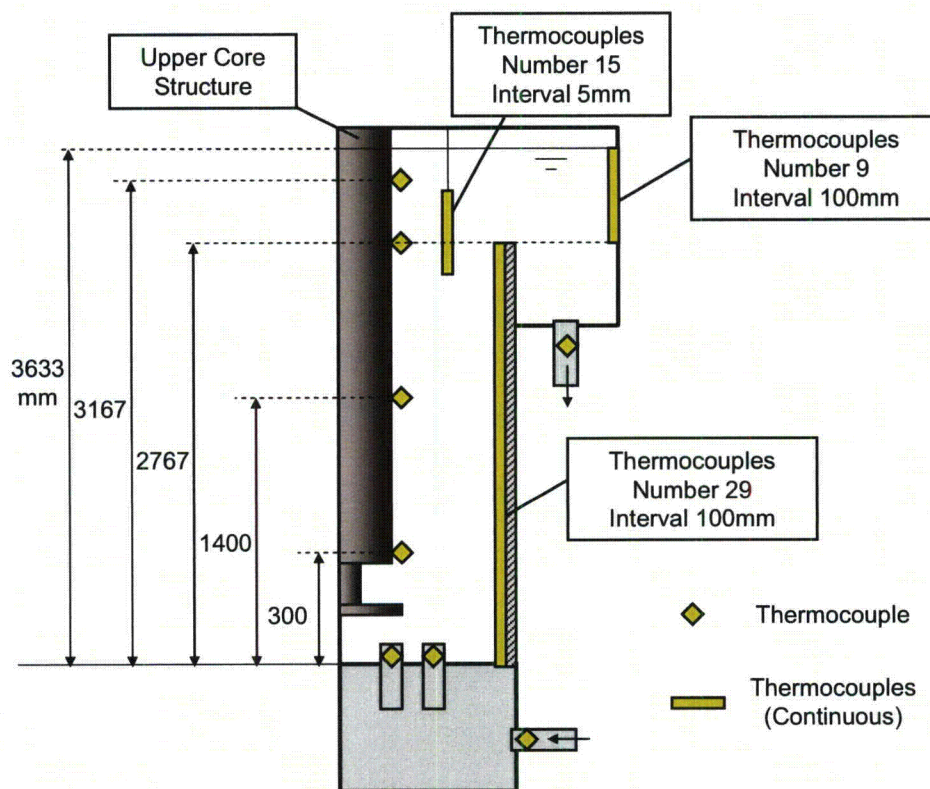


Figure 3-11 Points to obtain test data

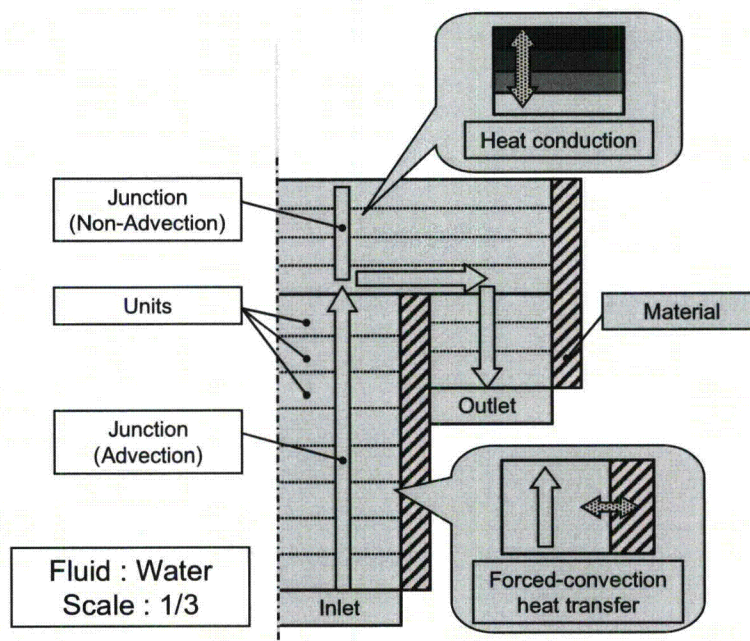


Figure 3-12 SAEMKON test model

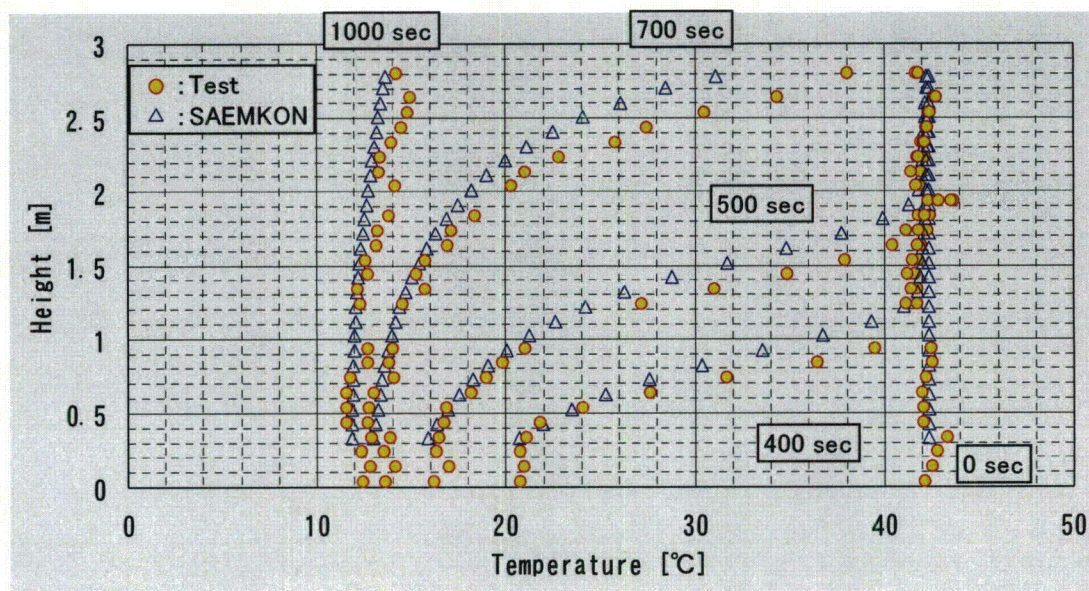


Figure 3-13 Axial temperature distribution (Case1)

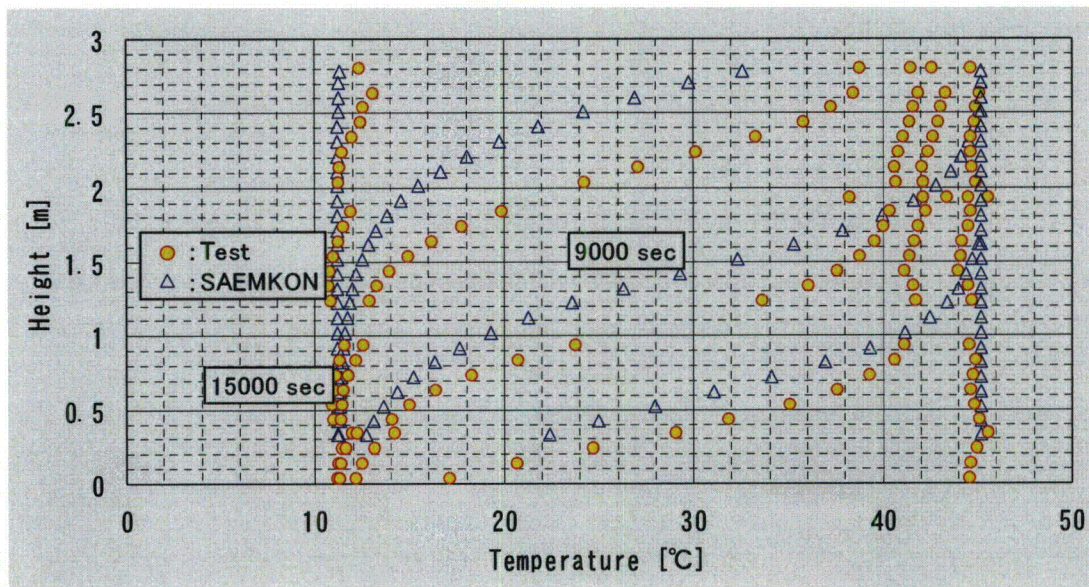


Figure 3-14 Axial temperature distribution (Case2)

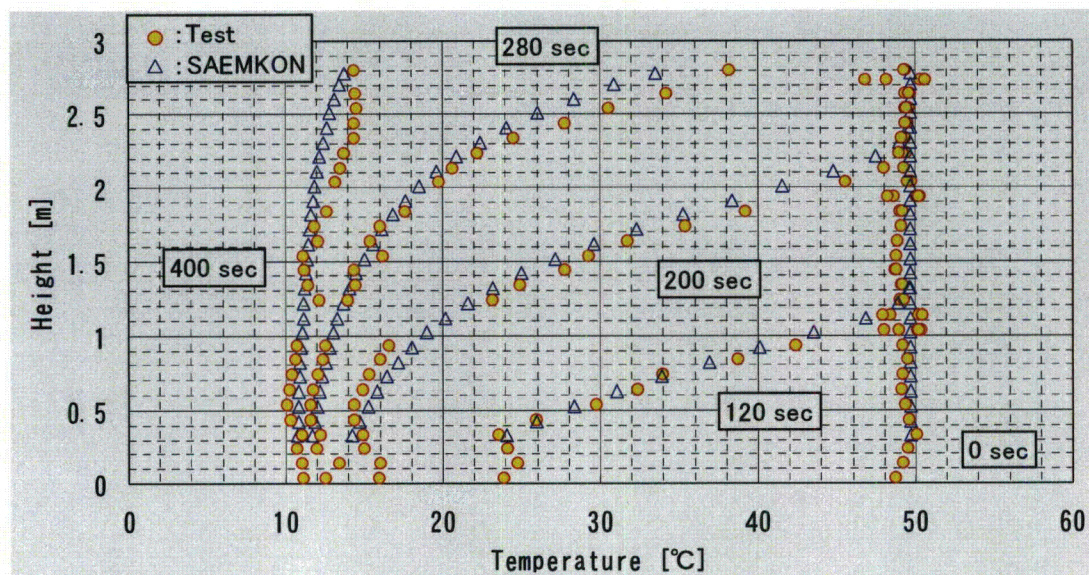


Figure 3-15 Axial temperature distribution (Case3)

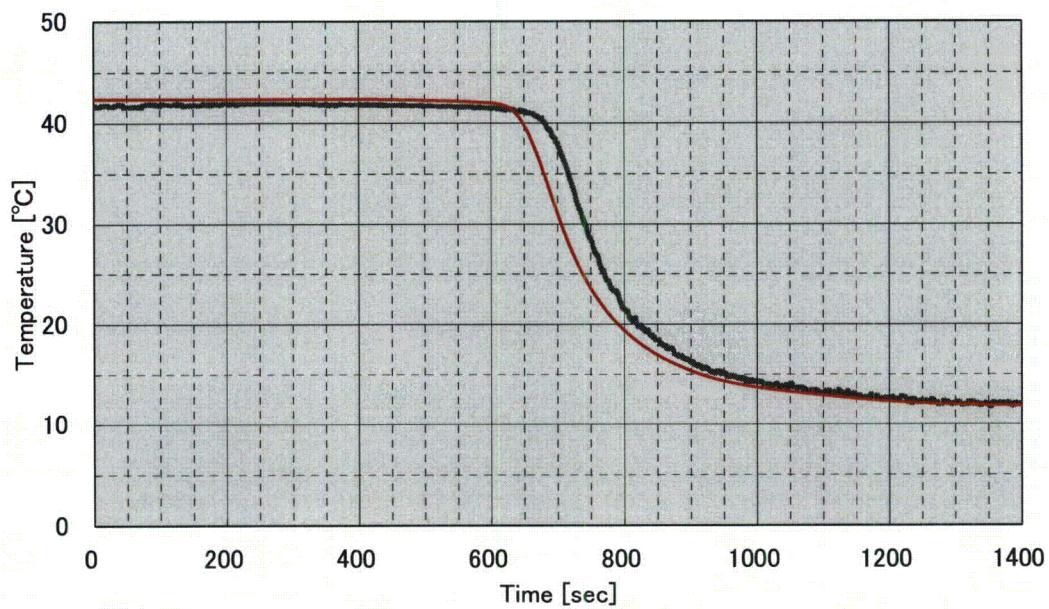


Figure 3-16 Temperature shift (Case1)

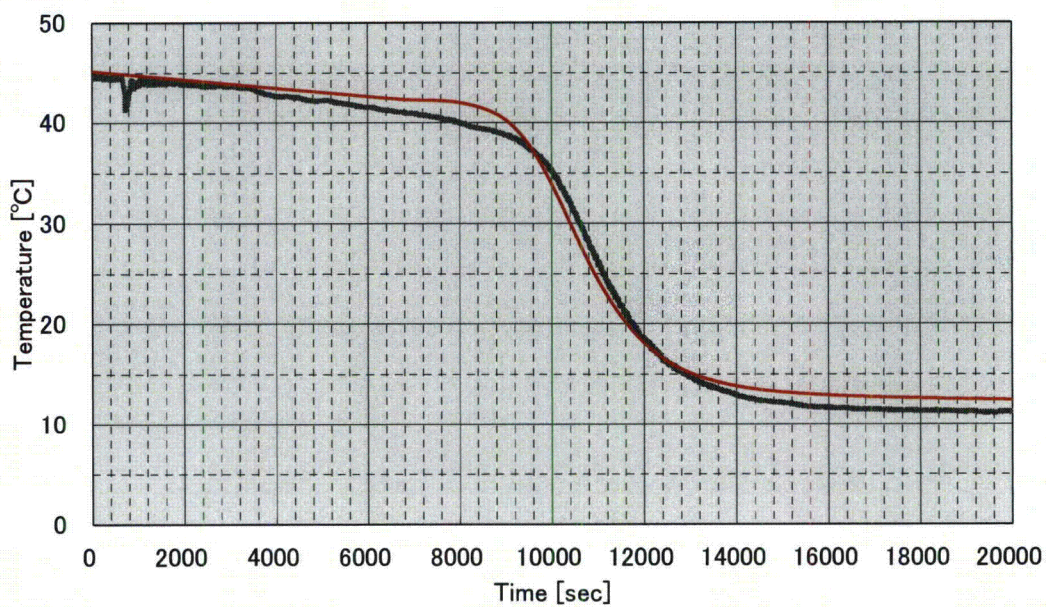


Figure 3-17 Temperature shift (Case2)

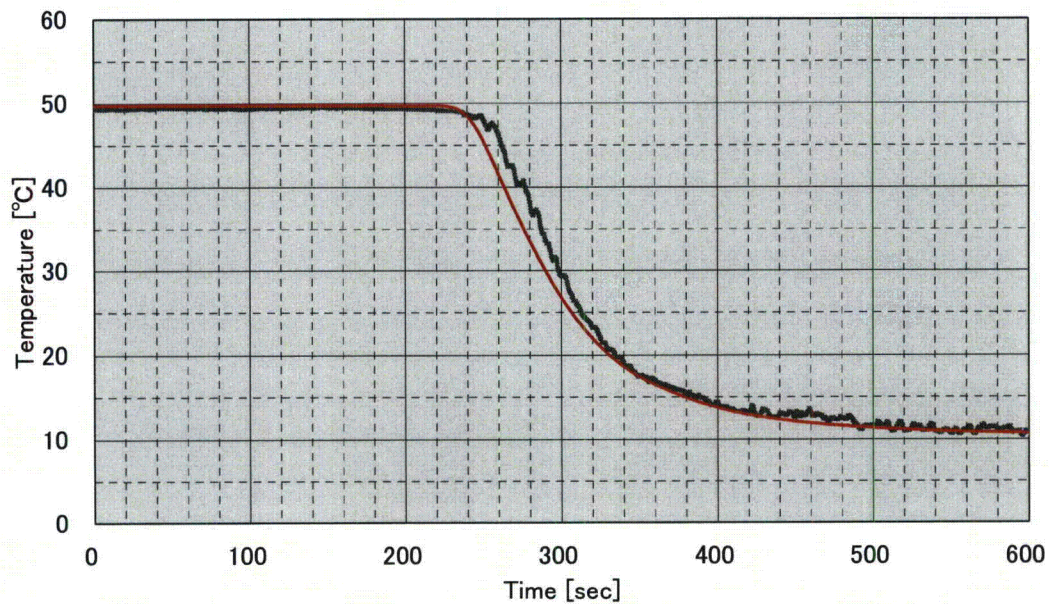


Figure 3-18 Temperature shift (Case3)

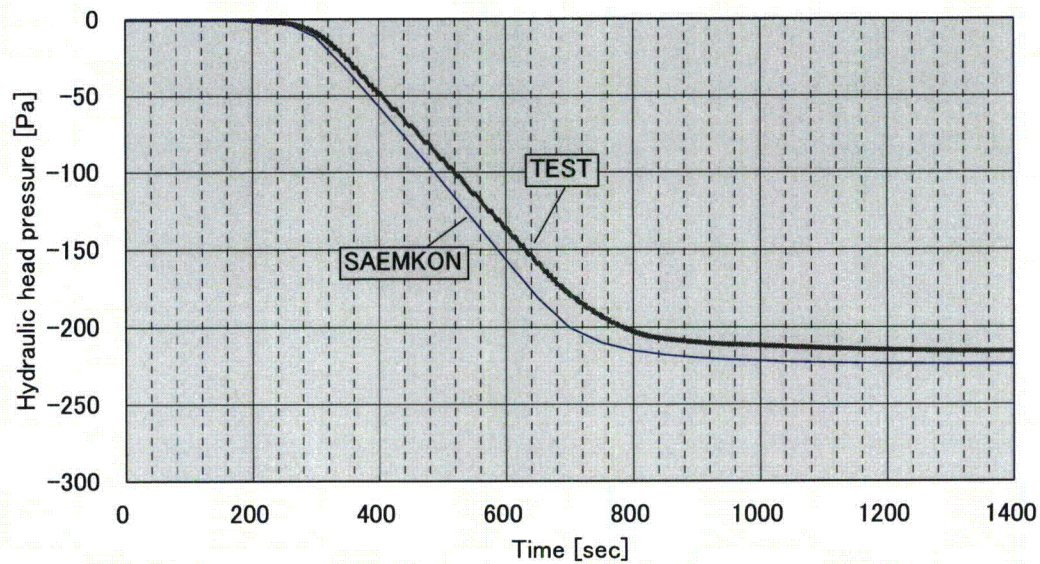


Figure 3-19 Comparison of hydraulic head pressure (Case 1)

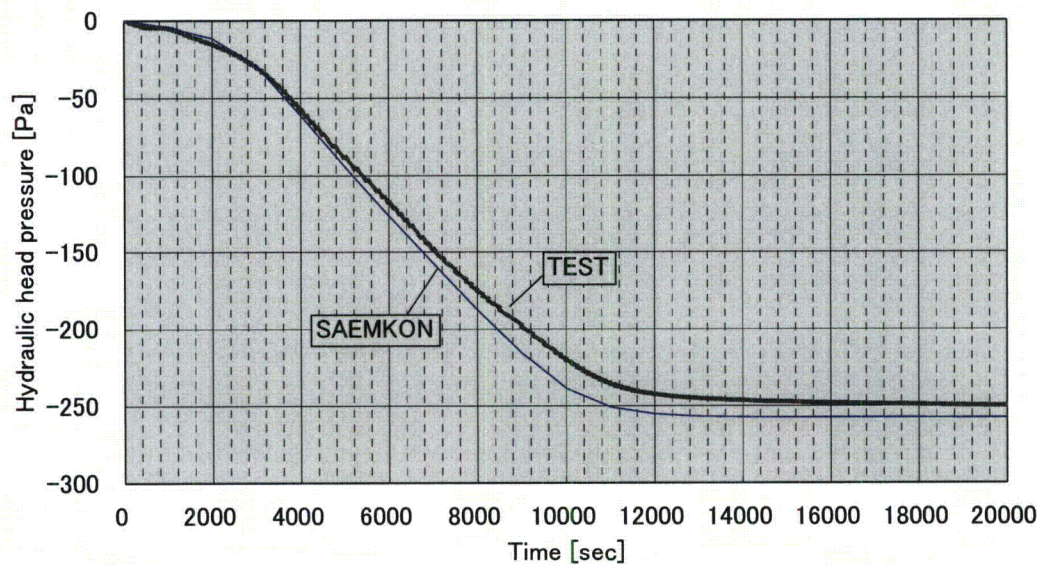


Figure 3-20 Comparison of hydraulic head pressure (Case 2)

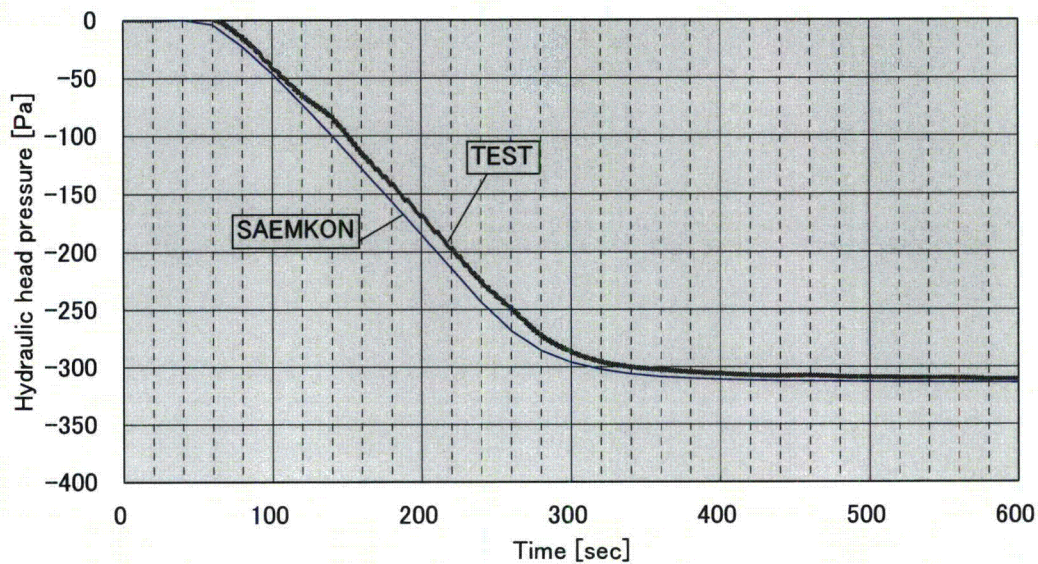


Figure 3-21 Comparison of hydraulic head pressure (Case 3)

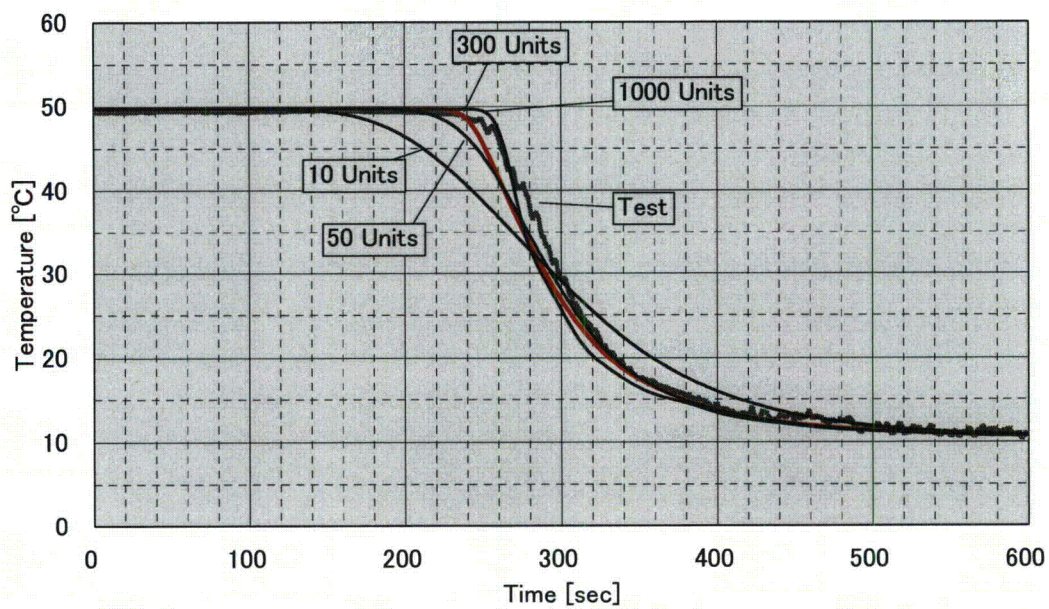


Figure 3-22 Effects of Nodalization

3.1.4. Heat transfer between tube and air of IRACS

(1) Phenomena description and validation objective

The chapter is concerned to heat removal of IRACS at the LOSP event. In a LOSP event, about 0.3 MW of heat is removed by the IRACS as shown in Figure 3-23. In the PIRT, heat transfers from the heat transfer tubes to the air outside the tube are identified as an important event. In this chapter, its validity is confirmed by considering the heat transfer coefficient of air side. Figure 3-24 shows AC flow during LOSP. The Re number is stable around 1000.

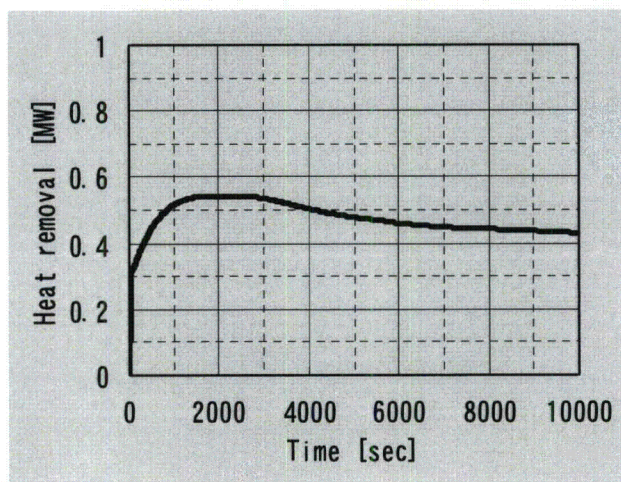


Figure 3-23 Heat removal of AC during LOSP

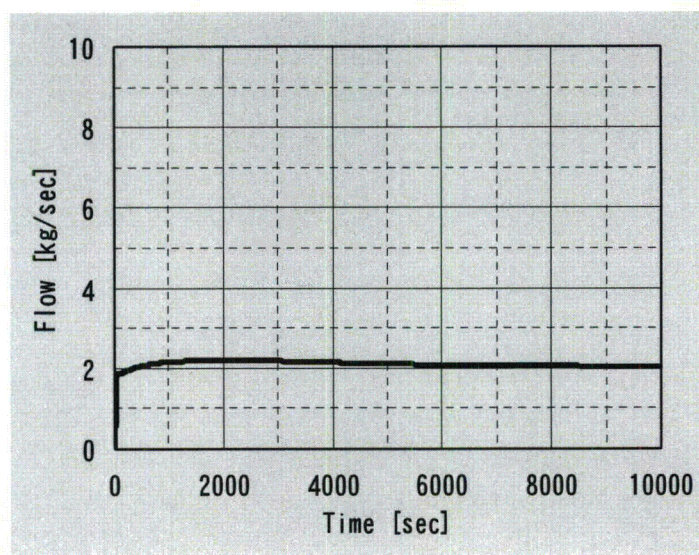


Figure 3-24 Flow rate of ACS during LOSP

(2) Test plan

The validation of this phenomenon will be performed with sodium test facility of Toshiba Corporation which has the same type of air cooler with 4S IRACS (Figure 3-25).

Table 3-4 shows the specification table for the Sodium test facility. Figure 3-26 shows the outline drawing for the Sodium test facility. Although the Re number of LOSP is around 1000, the test is performed in the range of 1000 to 15000 for the purpose of understanding the trend including maximum Re number 6000.



Air cooler

Figure 3-25 Sodium test facility of Toshiba Corporation

Table 3-4 Sodium Test Facility Specification Table

Primary (inside) fluid	Sodium
Secondary (outside) fluid	Air
Heat exchanger tube diameter	42.7mm
Heat exchanger tube thickness	2.8mm
Heat exchanger tube arrangement	Σ -type
Number of heat exchanger tube	8 (eight)
Length of Heat transfer tube (with Fin region)	0.95×4 m (per tube)
Fin thickness	2mm
Fin height	18.5mm
Fin pitch	5mm
Material of heat transfer tube and fin	SUS304

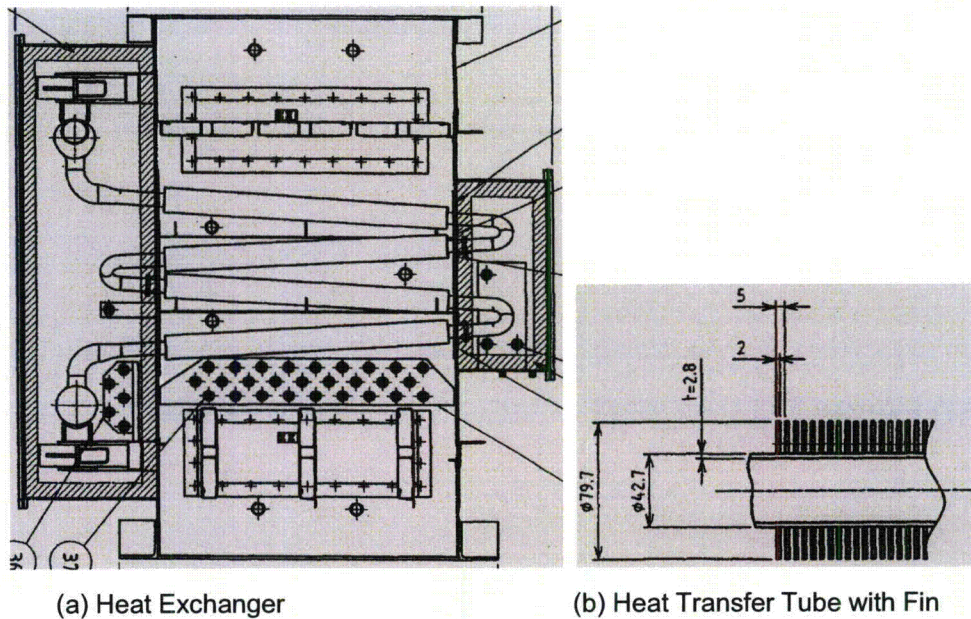


Figure 3-26 Sodium Test Facility Outline Drawing

As Table 3-5 shows, the test was planned to cover the range of Re number (1045-1210) during LOSP. The sodium test facility is modeled by SAEMKON as Figure 3-27 shows, and the analysis is performed.

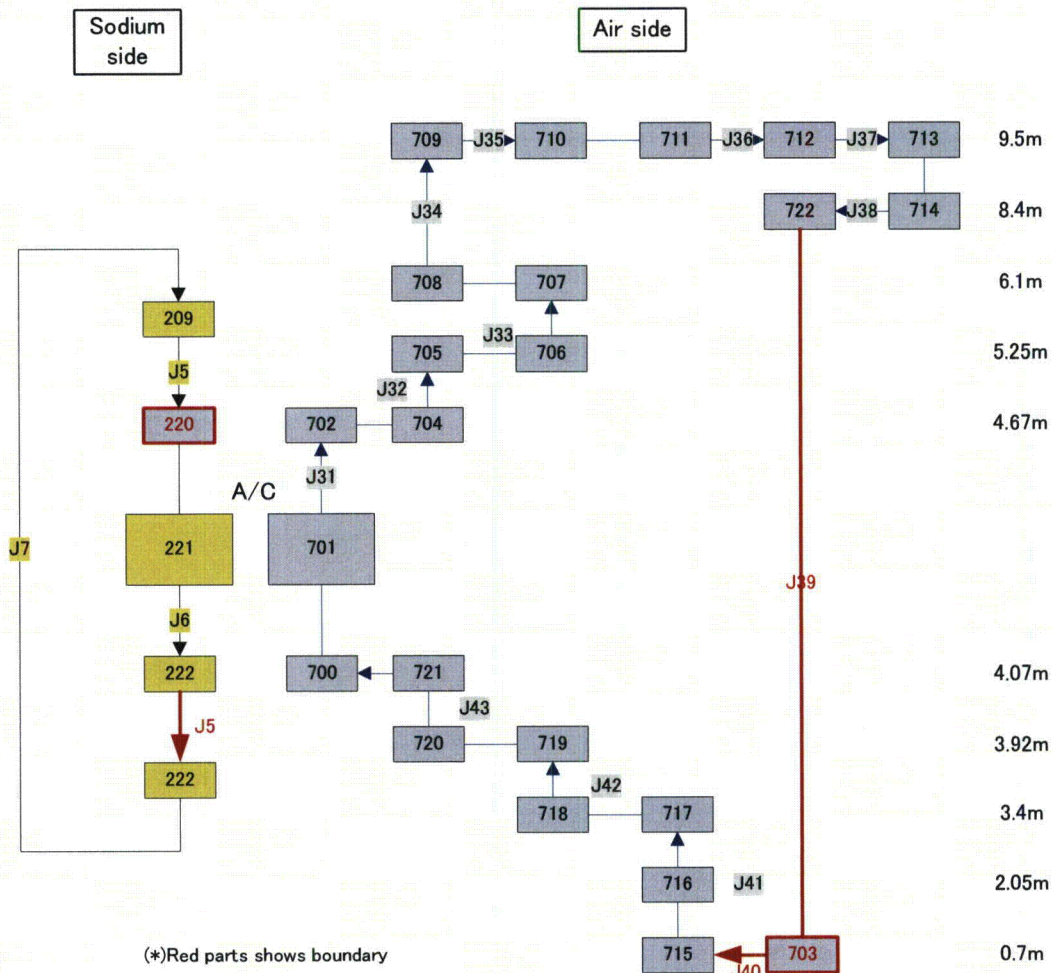


Figure 3-27 SAEMKON Sodium test facility model

Table 3-5 Test condition

No.	Sodium Flow rate	Temperature difference at Sodium inlet/outlet of air cooler	Air Re number (target value)	Air flow rate (target value)
	(L/min)	(deg. C)	(-)	(m3/min)
1-1	200	10	1000	19
1-2	200	14	1500	28
1-3	200	20	2500	46
2-1	300	7	1000	19
2-2	300	9	1500	28
2-3	300	13	2500	46
2-4	300	19	4000	74
2-5	300	24	6000	111
2-6	300	29	8000	149
3-1	400	14	4000	74
3-2	400	18	6000	111
3-3	400	22	8000	149
3-4	400	27	11000	204
3-5	400	32	15000	279

(3) Test result

The test results from the sodium test facility and SAEMKON results are shown in Figure 3-28. The results were obtained in the range from 997 to 16380 Re number and the range includes the target Re number. The tests No. a-1 and b-1 are performed with the condition of air natural circulation.

Figure 3-24 shows the comparison of sodium test and SAEMKON calculation results with heat transfer coefficient. According to these results, the SAEMKON heat transfer of IRACS is modeled correctly but not conservatively.

Table 3-6 Test Results

No.	Sodium Flow rate	Temperature difference at Sodium inlet/outlet of air cooler	Air Re number (target value)	Air flow rate	Sodium inlet temperature	Sodium outlet temperature	Air inlet temperature	Air outlet temperature	Cooling fan power
	(L/min)	(deg. C)	(-)	(m3/min)	deg. C	deg. C	deg. C	deg. C	%
a-1	191	10.2	997	19	286.1	275.9	22	138.5	0
a-2	193	15.5	1720	33	248.6	233.1	18.1	125.6	7
a-3	194	18.4	2682	51	215.4	197	16.6	102.5	12
b-1	289	8.2	1158	22	302.8	294.6	22.3	142.7	0
b-2	295	12.2	1791	34	279.1	266.9	19.1	139.5	6
b-3	295	15.3	2585	49	257.9	242.6	17.6	125.2	11
b-4	298	18.2	4114	78	236.3	218.1	16.2	100.7	18
b-5	300	20.5	6200	118	217.4	196.9	15.6	81.5	27
b-6	301	21.1	6954	132	213.2	192.1	19.1	79.7	31
b-7	302	22.4	8453	161	203.5	181.1	15.6	69.9	36
c-1	400	15.8	4070	77	263.2	247.4	17.9	114.6	18
c-2	407	18	6103	116	246.7	228.7	17.6	94.7	27
c-3	408	20.1	8312	158	234.9	214.8	17.7	82.4	36
c-4	412	22.3	11770	224	221.1	198.8	18.3	70.6	50
c-5	415	24.3	16380	311	208.8	184.5	18.9	60.9	69

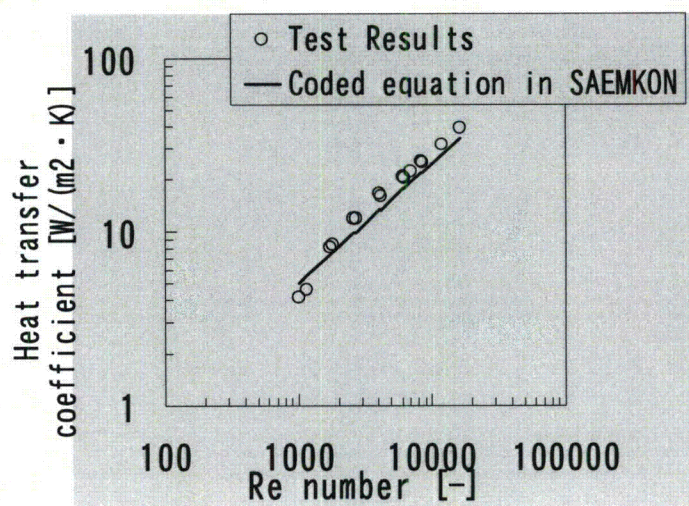


Figure 3-28 Heat transfer coefficient of test and SAEMKON

Also, the comparison of SAEMKON and the test is shown in Figure 3-29. Based on the result, SAEMKON can adequately evaluate the heat removal capacity among the range of Re number during LOSP.

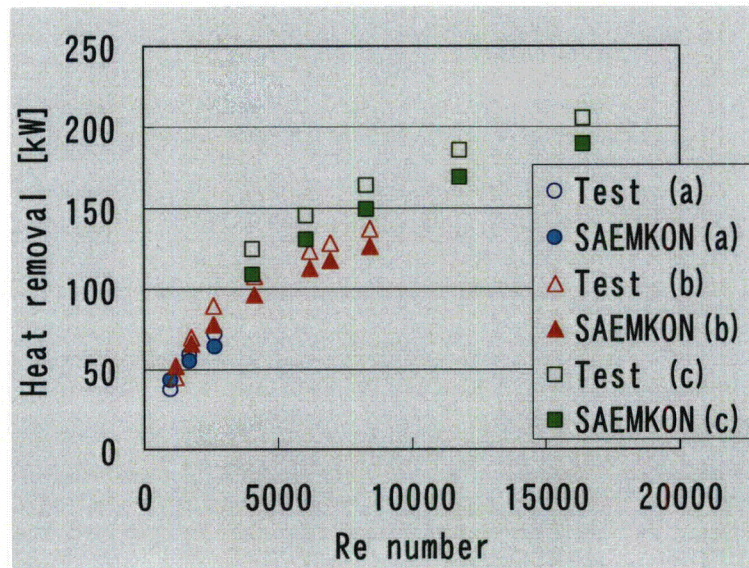


Figure 3-29 Comparison of SAEKMON and the test

(4) Consideration

For SAEKMON, a Jameson equation [11], to which compensation coefficient α is multiplied, is used.

$$Nu = 0.092 \cdot Re^{0.723} \cdot Pr^{1/3} \cdot \alpha$$

$(30^3 \leq Re \leq 10^5)$

In order to examine the effect of inaccuracy in heat transfer rates on the sensitivity of cladding tubes, compensation coefficient was used as a parameter. As Figure 3-30 shows, a parameter was set up to include the test data; $\alpha = 1/1.5$ and $\alpha = 1/0.9$. The results are shown in Figure 3-31 to Figure 3-33. The results confirmed that though it has some sensitivity for the outlet air temperature of ACS, it has low sensitivities for the secondary sodium temperature and cladding temperature; the maximum cladding temperature was within the ranges of plus and minus 5 deg. C. Accordingly, it is confirmed that the heat transfer model of the IRACS air is a reasonable agreement.

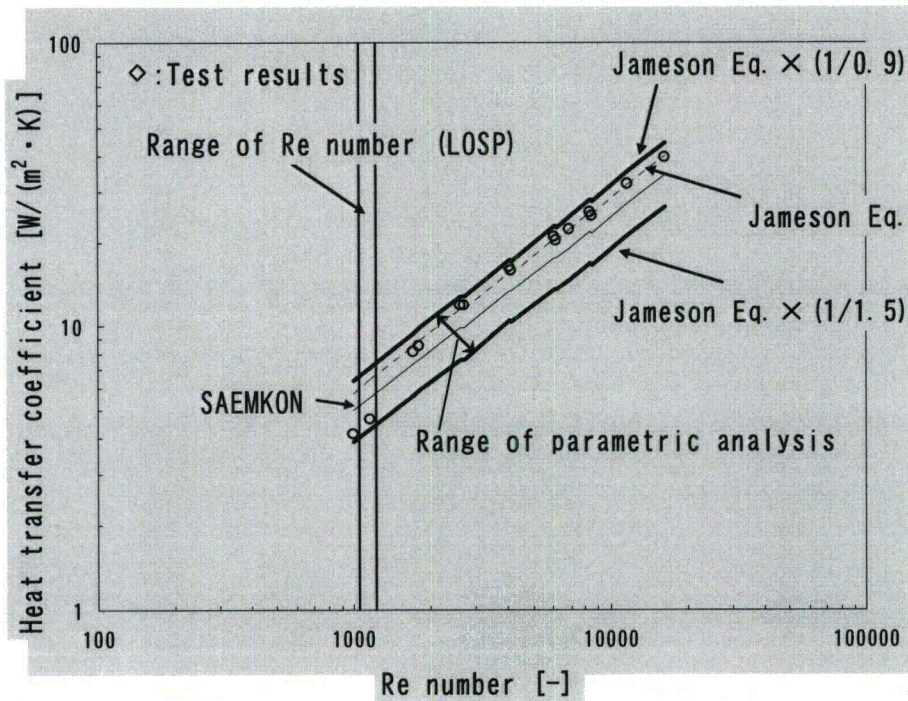


Figure 3-30 Compensation coefficient including the scope of the test

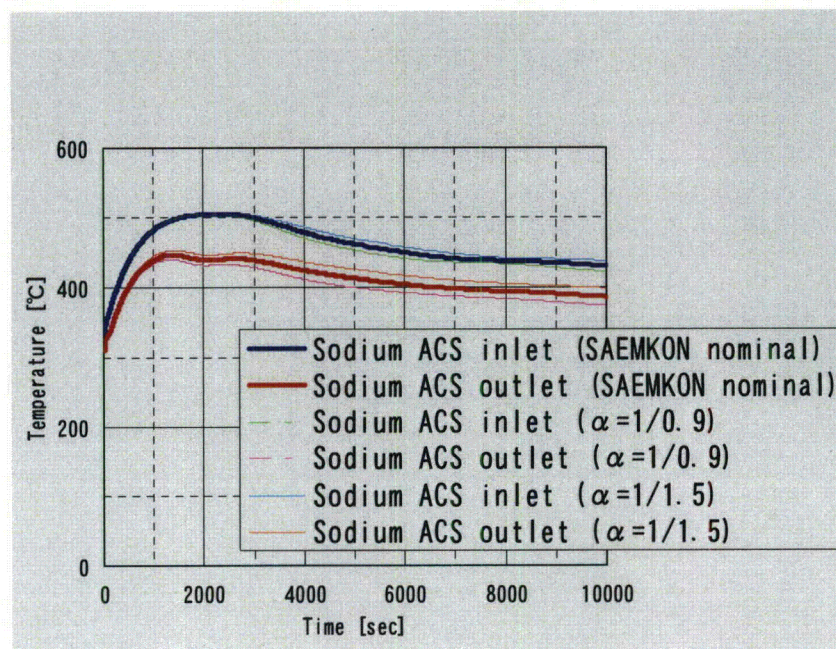


Figure 3-31 Sodium temperature at ACS inlet/outlet during LOSP

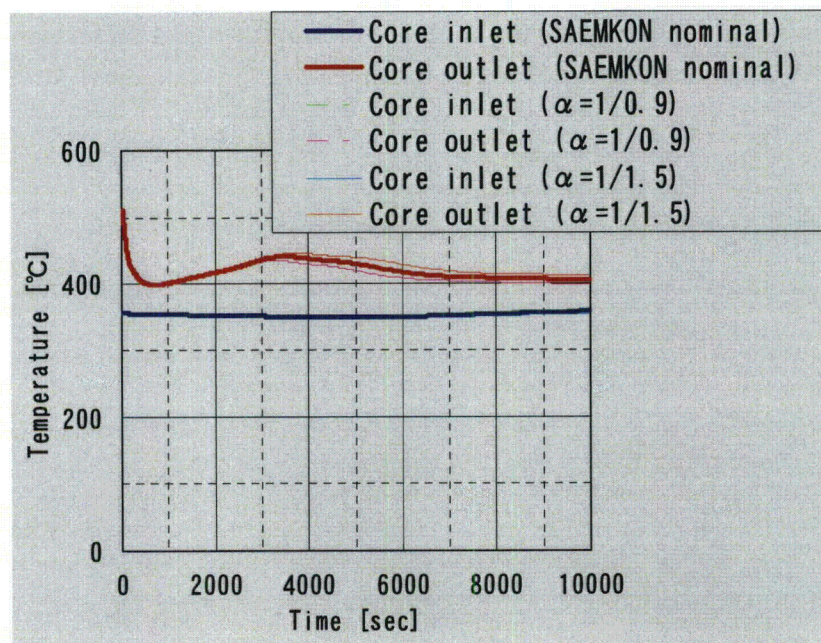


Figure 3-32 Sodium temperature at core inlet/outlet during LOSP

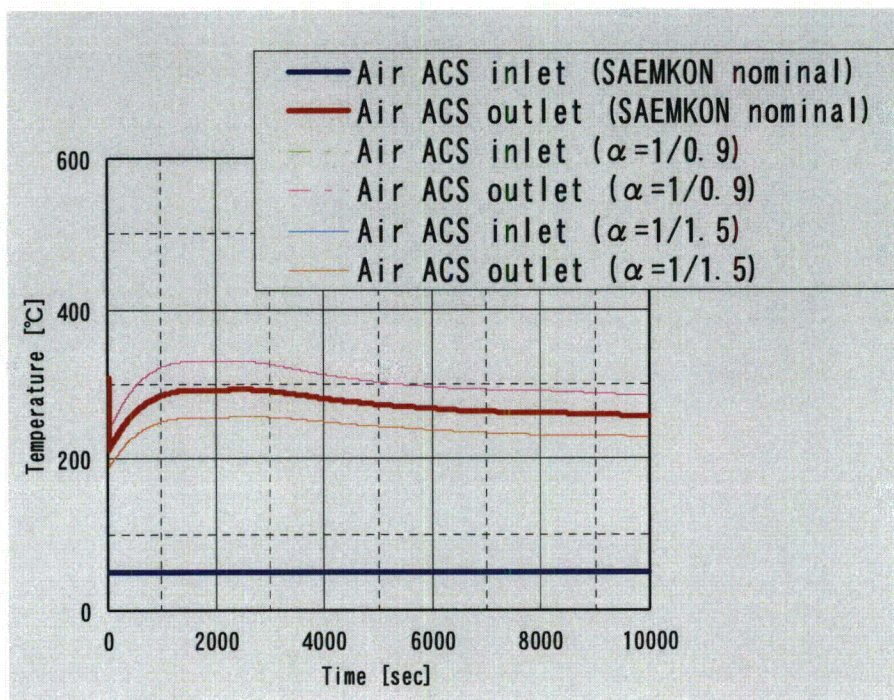


Figure 3-33 Air temperature at ACS inlet/outlet during LOSP

3.2. Integral Effects Tests

SAEMKON calculation has been performed for plant scale test. The effect of each phenomenon analyzed in Chapter 3.1 as SET is all summarized in this plant scale calculation. The overall system test is more complex than separate effect tests because the response is affected by interaction between models and phenomena.

In IET, analysis evaluation for experimental results on the plant is conducted and assesses the capability of SAEMKON to simulate the important phenomena selected in LOSP event.

The important phenomena are selected from PIRT and the following are classified as IET:

- Natural convection in reactor system
- Natural circulation in primary heat transport system
- Natural circulation in intermediate heat transport system.

Among the phenomena, analysis results for “Natural circulation in primary heat transport system” are described in this chapter. The purpose of this validation is to confirm the capability of SAEMKON to simulate natural circulation behavior of the plant.

3.2.1. Natural circulation in primary heat transport system

3.2.1.1 Phenomena description and validation objective

Natural circulation is driven by natural circulation head and pressure losses along the natural circulation path. The natural circulation head is determined by temperature difference between heat source and heat sink. As for natural circulation head in primary system of 4S, the main heat source is core and heat sink is IHX and RVACS. The pressure losses along the path are the summation of pressure losses due to wall friction, flow contraction, flow expansion and all the local phenomena relevant to buoyancy-driven flow.

The test analysis is conducted with experimental data of the Experimental Breeder Reactor (EBR)-II to simulate the natural circulation behavior. In this analysis, flow rate and coolant temperature in core region are evaluated as validation parameters.

3.2.1.2 Test Description

Test analysis of the Shutdown Heat Removal Test (SHRT)-17 in the EBR-II was chosen to experimentally validate SAEMKON [12, 13, 14]. EBR-II is a small reactor tank system which uses metal fuel same as 4S, and more than 600 subassemblies are placed within the core. The SHRT-17 test is a protected loss of flow test which demonstrates natural circulation behavior and has the lowest minimum transient coolant flow rates of any SHRT tests. A comparison table between 4S and EBR-II is shown in Table 3-7 [15, 16].

The SHRT-17 test started from full power and full flow. Then the main primary pumps and the intermediate loop pump tripped and the reactor was scrammed. At the same time, pumps started coast-down and the transient involved forced convection during the initial steady-state. After the pumps flow coast-down stopped, the test transitions into natural circulation. EBR-II had an auxiliary pump in the primary loop to minimize the severity of an accident, such as loss of power to main pumps, but it was shut off for the SHRT-17 test.

For SHRT-17 test, detailed coolant temperature and flow rate data are available from thermocouples and flow meters instrumented in the subassembly, called XX09. The XX09 is nearly identical to an MK-IIA driver-fuel type subassembly which contains 91 pins. Although, XX09 which contains 61 pins for the outer row of pins are replaced to thimble flow region which contains sodium with a small flow rate [12]. Therefore XX09 has another wall in addition to usual ductwall. XX09 includes subassembly wall containing 61 pins and thimble wall containing thimble flow region surrounding the subassembly wall. Within the subassembly wall, a total of 28 thermocouples were placed in the coolant near the cladding

at different axial and radial locations. Also, two flow meters are located in series below the fuel region of subassembly. Figure 3-34 shows the description of XX09 subassembly.

Reynolds number in XX09 subassembly and Grashof number can be evaluated from the experimental data. In the natural circulation of this SHRT-17 test, Reynolds number exists in the range from 4.7×10^2 to 1.2×10^3 and Grashof number from 4.2×10^{15} to 7.9×10^{15} . On the other hand in 4S LOSP event, Reynolds number in core region exists in the range from 3.5×10^2 to 2.3×10^3 . At the same time, Grashof number exists in the range from 7.5×10^{15} to 4.1×10^{16} . The regions of Reynolds number give close agreement with 4S LOSP event. As for Grashof number, the region of 4S shows greater than that of EBR-II. This is because the height between heat source and heat sink of 4S is three times higher than that of EBR-II, although heat flux of 4S is smaller in an order of magnitude.

The detail data regarding the reactor and the test were provided from Argonne National Laboratory (ANL).

Table 3-7 Comparison between 4S and EBR-II [15, 16]

Item	Unit	4S	EBR-II
Power	MWt	30	62.5 (SHRT17: 60.5)
Core Height	m	2.5	0.343
Core Diameter	m	0.95	1.562 (including blanket) 0.679 (excluding blanket)
Fuel	-	U-Zr metal alloys	U-Zr metal alloys
Reactor Height	m	23.4	12.14
Core Inlet/Outlet Temperature	deg-C	355 / 510	371 / 473
Primary Flow rate	kg/s	152	500
Pump	-	Electromagnetic Pump	Mechanical Pump
Configuration	-	Tank	Tank
Spacer	-	Wire	Wire
No. of pins per assembly	No.	169	91
Natural Circulation Behavior			
Re number	-	$3.5 \times 10^2 \sim 2.3 \times 10^3$	$4.7 \times 10^2 \sim 1.2 \times 10^3$
Gr number	-	$7.5 \times 10^{15} \sim 4.1 \times 10^{16}$	$4.2 \times 10^{15} \sim 7.9 \times 10^{15}$

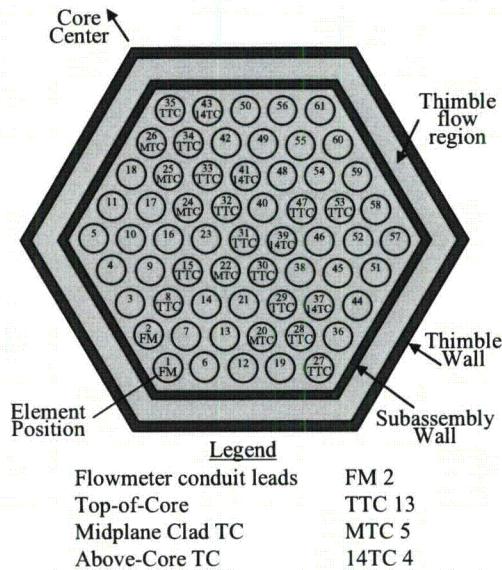


Figure 3-34 XX09 subassembly[12]

3.2.1.3 Analysis model

The nodalization scheme for the primary system in EBR-II is shown in Figure 3-35 [17]. The primary system is located in a large primary tank described with one unit. The principle components of the primary system are the core, two main pumps, and a single IHX. The pipes connecting these components are modeled with several units. The detailed description of setting on each component and important phenomena are as follows.

(1) Power and Removal heat

The normalized power is obtained as measured data in the SHRT-17 test. In the analysis, those data are directly used as an input data of power change.

On the other hand, validation target of this analysis is only applied to primary system and so IHX is the primary component through which decay heat removal takes place. Therefore, temperature and flow rate of coolant at IHX inlet in the intermediate heat transport system is set as boundary condition.

(2) Core channel

The core is modeled with 17 channels. Subassemblies which show similar characteristics are put into one channel. As for XX09 and its six neighbors, each subassembly is modeled separately to express the temperature and flow rate more precisely. The thimble region, located internally in XX09 subassembly, is not modeled within the channel. Instead, flow path is located around the XX09 subassembly channel to render the region.

(3) Pressure loss in core region and pipes

The orifice pressure loss and frictional pressure loss can be modeled in both core flow region and sodium flow pipes. The frictional pressure loss is expressed in a function of Reynolds number. Different coefficients can be defined in each channel at core flow region and in each unit at sodium flow pipes. As for sodium flow pipes, bend pressure losses are also included within the frictional pressure loss.

(4) Radial heat transfer between subassemblies

Radial heat transfer in core region is considered only between XX09 and its six surrounding assemblies. At this time, flow velocity and heat capacity of the thimble region are also considered. Therefore the Nusselt number modeled in the form depending on both the Reynolds number and the Prandtl number is used in the heat transfer between thimble region and ductwall of XX09 and its surrounding subassemblies.

(5) IHX

In the analysis of natural circulation behavior, axial distribution of IHX temperature has a significant effect on natural circulation head. It is confirmed from the evaluation that 100 axial partition of IHX is enough to simulate the natural circulation behavior of this test. Therefore IHX is axially divided into 100 partitions in this test analysis.

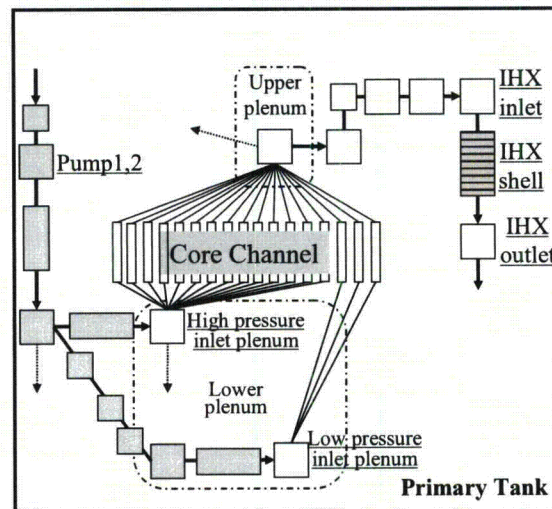


Figure 3-35 Flow network model of EBR-II in SAEMKON

3.2.1.4 Calculation Results

The comparison between analytical results and experimental data are discussed in this

chapter. The target for comparison is coolant flow rate and coolant temperature in XX09 subassembly.

Figure 3-36 shows a comparison of the transient coolant flow rate of the XX09 subassembly in SHRT-17. In the XX09 subassembly, two flow meters were provided in series below the fuel region and the measured data differed after the flow coast-down stops. This is because of the uncertainty width in the flow meter in low flows. The calculated flow rate is roughly in accordance with measurements of upper flow meter.

Figure 3-37 through Figure 3-39 show a comparison of the average coolant temperature in three different elevations of the XX09 subassembly. The coolant temperature was measured with thermocouples described with three different denotations of TTC, MTC, and 14TC, which indicate the axial locations of near the top of the fuel, middle of the core and above the fuel in the gas plenum region respectively.

According to these results, the calculated temperature predicted the measured values correctly. Among the calculated temperatures, MTC shows conservative behavior almost all through in the transient time within 600 sec. On the other hand, the predictions of TTC and 14TC, which located in the upper part and show higher temperature in core region, show apparently lower than the measured data in the transient time from about 50 sec to 300 sec.

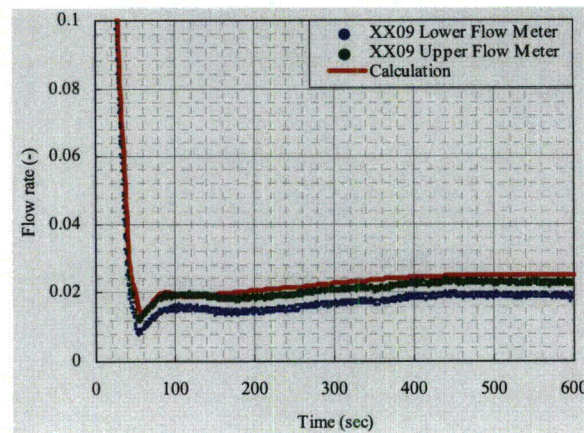


Figure 3-36 Comparison of coolant flow rate

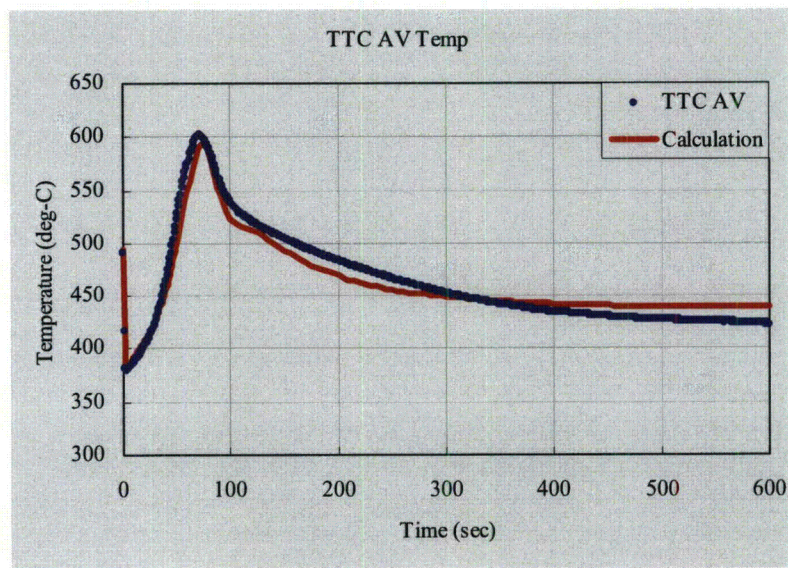


Figure 3-37 Comparison of coolant temperature (TTC)

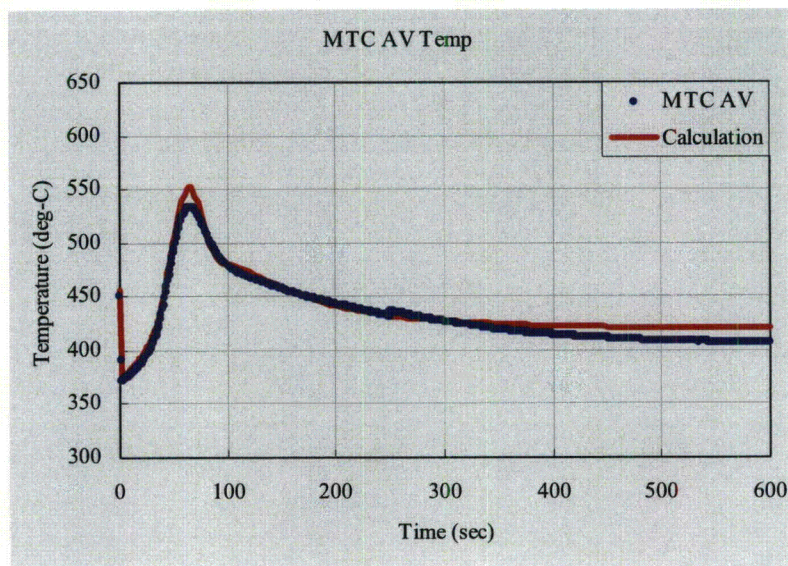


Figure 3-38 Comparison of coolant temperature (MTC)

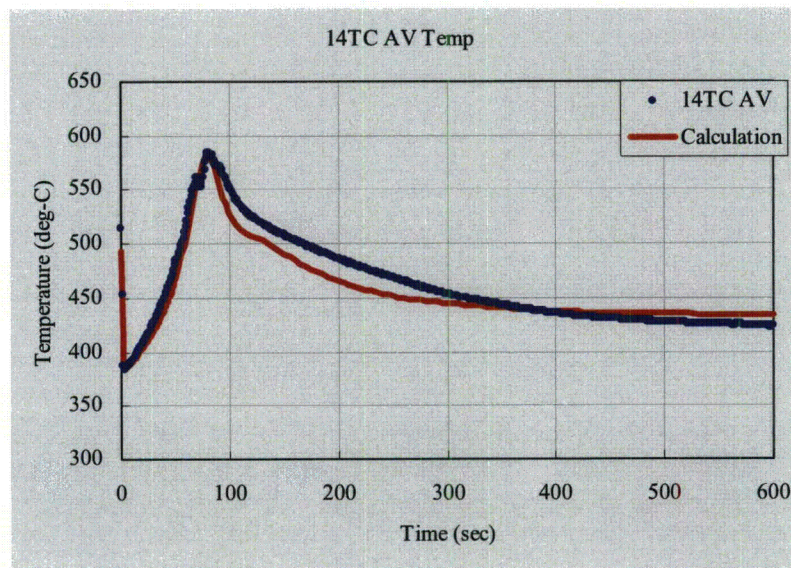


Figure 3-39 Comparison of coolant temperature (14TC)

3.2.1.5 Consideration

As a result, analytical result shows good agreement with experimental data. As described in the previous chapter, SAEMKON simulates the SHRT-17 test in EBR-II correctly. For coolant peak temperature appeared near 75 seconds, the calculation temperature shows higher than the measurement and predicts the test conservatively at MTC. On the other hand, calculated peak temperature at both TTC and 14TC show lower than the measurement. The difference between these measured data and calculated data are within the range of safety factor which is explained below. Therefore, prospect of the analytical capability of SAEMKON to natural circulation behavior of SHRT-17 in EBR-II could be confirmed.

Here, 'the range of safety factor' mentioned above is the difference within 25°C to the measurement. At low flows as appeared in this test, flow meter reading shows the error about 10% of the reading [12]. The error of coolant temperature can be estimated from this flow reading error and difference between inlet and outlet temperature of the subassembly. As a result, the coolant temperature error is obtained as 25°C and this value is used to the range of safety factor.

4. CONCLUSION

The validation of the TOSHBA self-developed safety analysis code SAEMKON for LOSP event has been performed as shown in Table 4-1.

In SET phase, the analysis results of the important phenomena have been evaluated with water hydraulic test, data of sodium test facility and published data. "Pressure loss in core region", "Natural convection in core region" and "Coolant mixing effect in upper plenum including thermal stratification" were evaluated as good agreement. "Heat transfer of IRACS between tube and air" was evaluated as reasonable agreement.

In IET phase, the test data of EBR-II were used and the capability of the code to simulate natural circulation behavior of the plant has been confirmed. The results of SAEMKON were evaluated as good agreement.

Above the results, the capability of SAEMKON in LOSP was confirmed and the validation of this event was performed. The important phenomena were evaluated with tests data and published data and all of the results showed acceptable agreement.

Table 4-1 Validation Results

Matrix		TEST TYPE			
		S		I	
		Water hydraulic test	Data of sodium test facility	Published data	EBR-II
Phenomena	Pressure loss in core region (inter-assembly flow distribution)	—	—	●	—
	Natural convection in core region	—	—	●	—
	Coolant mixing effect in upper plenum including thermal stratification	●	—	—	—
	Heat transfer of IRACS between tube and air	—	○	—	—
	Natural convection in reactor system	●	—	●	●
	Natural circulation in primary heat transport system	—	—	—	●

5. REFERENCES

- 1 S., HATTORI, N., HANDA, "Use of Super-Safe, Small and Simple LMRs to Create Green Belts in Desertification Area" Trans. ANS., Vol.60 (1989)
- 2 TOSHIBA CORPORATION, "4S Safety Analysis", ADAMS, ML092170507, (2009)
- 3 TOSHIBA CORPORATION, "Phenomena Identification and Ranking Tables (PIRTs) for the 4S and Further Investigation Program – Loss of Offsite Power, Sodium Leakage from Intermediate Piping, and Failure of a Cavity Can Events," ADAMS, ML101400662, (2010)
- 4 NUREG 1737, "Software Quality Assurance Procedures for NRC Thermal Hydraulic Codes", December 2000.
- 5 NUREG 0800, "Standard Review Plan for the Review of Safety Analysis Reports for Nuclear Power Plants," Chapter 15.0, Accident Analysis, March 2007.
- 6 F. Namekawa, et.al., "BUOYANCY EFFECTS ON WIRE-WRAPPED ROD BUNDLE HEAT TRANSFER IN AN LMFBR ASSEMBLY", American Institute of Chemical Engineers, No.236, Vol 80 page 128-133, 1984
- 7 Suzuki, T. et al., 1983, Natural circulation test in experimental fast reactor 'JOYO', J. At. Energy Soc. Jpn. 25(9). 729-738
- 8 Sawada, M. et al., 1990, Experiment and analysis on natural convection characteristics in the experimental fast reactor JOYO, Nucl. Eng. Des. (Netherlands). 120 341-347
- 9 Mochizuki, H., 2007, Inter-subassembly heat transfer on sodium cooled fast reactors; Validation of the NETFLOW code, Nuclear Engineering and Design, 237(19), 2030-2053
- 10 N. Usui, et.al., "Thermal Hydraulics Test for Validation of 4S Safety Analysis Code ARGO", Paper 11047, ICAPP 2011
- 11 Donald Q. Kern, "PROCESS HEAT TRANSFER", Tata Mc Graw Hill, Page 555, 1997

- 12 F. E. DUNN et al., "Whole Core Sub-Channel Analysis Verification with the EBR-II SHRT-17 Test," Proceedings of the International Congress on Advances in Nuclear Power Plants (ICAPP'06), paper-6255, Reno, NV USA (2006)
- 13 F. E. DUNN et al., "Verification and Implications of the Multiple-pin Treatment in the SASSYS-1 Liquid-Metal Reactor Systems Analysis Code," Nuclear Technology, Vol.114, pp. 147-157 (1996)
- 14 Y. NISHI et al., "Verification of the plant dynamics analytical code CERES; Comparison with EBR-II Tests," Proceedings of the International Congress on Advances in Nuclear Power Plants (ICAPP'10), paper-10271, San Diego, CA, USA (2010)
- 15 "Fast Reactor Database 2006 Update," IAEA-TECDOC-1531, IAEA (2006)
- 16 G.H.GOLDEN, "Evolution of thermal-hydraulics testing in EBR-II," Nucl. Eng. Design., 101, Page 3-12 (1987)
- 17 F. SEBE et al., "Validation of a plant dynamics code for 4S – Test analysis of natural circulation behavior -," Proceedings of the International Congress on Advances in Nuclear Power Plants (ICAPP'12), paper-12294, Chicago, USA (2012)